Sezione di Milano

INFN/TC–93/06
9 Giugno 1993

M. Canali, L. Rossi:

DYNQUE: A COMPUTER CODE FOR QUENCH SIMULATION IN ADIABATIC MULTICOIL SUPERCONDUCTING SOLENOIDS

Servizio Documentazione
dei Laboratori Nazionali di Frascati

INFN – Istituto Nazionale di Fisica Nucleare
Sezione di Milano

INFN/TC–93/06
9 Giugno 1993

DYNQUE: A COMPUTER CODE FOR QUENCH SIMULATION IN ADIABATIC MULTICOIL SUPERCONDUCTING SOLENOIDS

M.Canali L.Rossi
INFN – Sezione di Milano, Laboratorio LASA and Dipartimento di Fisica dell'Università di Milano, via fratelli Cervi 201, 20090 Segrate (MI), Italy

ABSTRACT

Several activities on applied superconductivity and related techniques have been developed at LASA for some years. In particular studies and measures on the quench propagation velocity in adiabatic, superconducting coils have been carried out in relation to the design and construction of the 18 tesla superconducting facility *SOLEMI* These studies aim to understand the quench evolution and its effects, which is the main point in order to design adequate protection systems for these sort of magnets.

A useful tool to achieve these tasks is our computer code *Dynque* which is specific for quench simulation. The code is able to predict the resistive zone growth , the current decay, the terminal voltages and the hot spot temperature during a quench event in multicoil and multisection magnets.

In this paper a thoroughly description of the code will be given, the approach and the approximations used to evaluate the different quantities will be discussed and some examples of the simulations compared with experimental results will be shown.

1 INTRODUCTION

When a region of a superconducting magnet gets normal, the Joule heat produced in the normal zone, if not removed, propagates because of thermal conduction and, under certain conditions, it may cause the surrounding zones to quench and, in a sort of chain process, all the coil may get normal. During this process the magnet resistance increases because of the growth of the resistive volume and of the increase of temperature and the magnet can eventually experience too high voltages and dangerous stress levels induced by thermal gradient.

Even if the current is well below its critical value, there are a lot of disturbances which may cause a magnet to quench, in particular the mechanical ones can't be fully controlled and avoided. An epoxy impregnated winding, in which the normal zone spreads essentially in an adiabatic way, is more susceptible to quench and, in this case, almost all the energy stored in the magnetic field is dissipated inside the coil. Therefore a magnet design must permit a quench without any risk for the system, and whatever protection is used the knowledge of the effects produced by the quench is required. Information about it may be obtained by studying small scale models but to be really significant the models must be often complex and expensive systems.

Instead of making experimental tests on prototypes it is possible to achieve very useful information in a faster and cheaper way by using a simulation code able to predict all the quantities of interest during a quench event. In this way it's very simple to change something in the geometry or in the electric circuit and find the best configuration.

For these reason the code *Dynque* has been developed in the lab and several sets of measurements have been carried out. The comparison between experiments and simulations has been very useful both to test the code and, mainly, to work out the effective quench velocities.

First the description of the theoretical approach to the problem is given, then the main parts of the program are described; finally the way we used *Dynque*, together with the experiments to obtain the values for the quench velocities, is discussed.

Hereinafter we'll call magnet any independently supplied system of n coils ($n \geq 1$) connected in series to each other; winding will be used as a synonym of coil and if a coil is provided with voltage taps we'll call section any volume between two consecutive voltage taps.

2 THE CODE DYNQUE: GENERAL FEATURES

The quench simulation program has been developed with the following features:

- Capability to predict the effects of a quench event in multiple adiabatic solenoids, like *SOLEMI* ,in which several coils wounded with cables made of different materials (typically NbTi and Nb_3Sn) may be electrically connected.

- Possibility to evaluate voltages between intermediate voltage taps each coil may be provided with. As it will be widely discussed in the following chapters, this is a very important option in order to study the quench propagation velocities in transverse direction.

- A flexible structure which allows to change or modify the evaluation of a single quantity leaving the others unchanged so that the program might be easily improved, if it's necessary. Actually different formulations for quench propagation velocity may be used in order to compare simulations and experimental results.

In this chapter the flow–chart of the program is discussed, leaving to the following chapters a detailed discussion about the structure of each subroutine, how the different quantities are worked out and what approximations have been used. In order to achieve flexibility, the computer program is conceived like a collection of subroutines, each one having a particular target or calculating a particular quantity, linked together by the main program. Fig.1 shows the *Dynque* flow–chart.

The input data are read by the subroutine SUBREAD and they are:

- Number of temporal steps and time increment to be used.

- Number and geometric dimensions of the windings.

- Number and position of the voltage taps.

- Time and position of the quench starting point.

- Operating current, critical current of the cable and magnetic field in locations which will be later specified.

- Self and mutual inductances.

- Cable components and their percentage in the unit cell.

- Information about the electric circuit: dumping resistance, delay time, arc time, maximum voltage of the power supply, number of magnets electrically connected in series and independently supplied.

An example of the input file is reported in the last section, after the list of symbols.

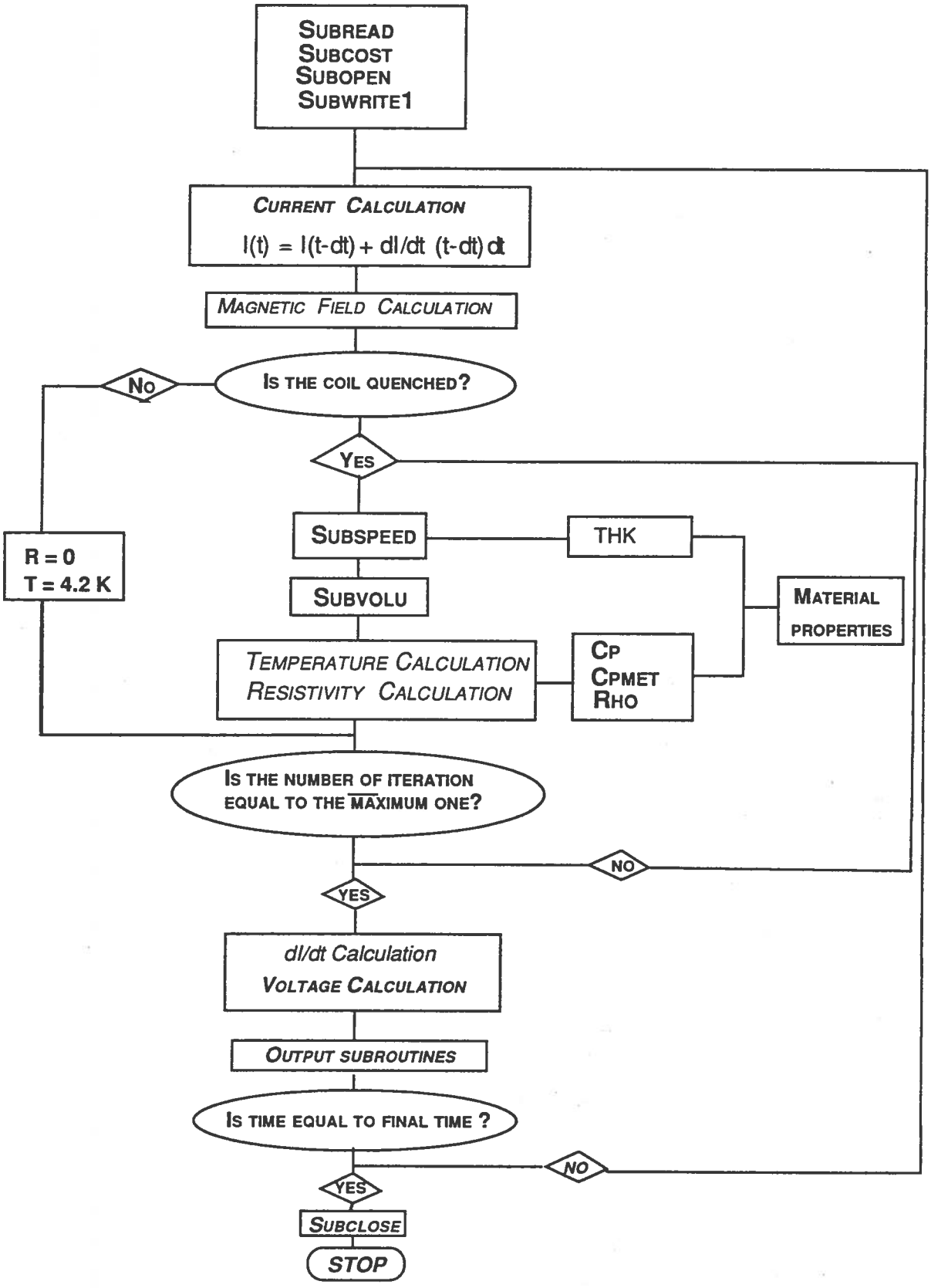

FIG. 1: Flow–chart of the computer code DYNQUE

After the input data reading, the output files are opened by the subroutine SUBOPEN, headed by SUBWRITE–1, while some constants used in the program are cal-

culated by SUBCOST. At this point the first temporal loop starts. At first the current I(t) and the magnetic field on each winding are calculated. Then, if a coil is quenched, the quench propagation velocities in longitudinal, axial and radial direction are evaluated by SUBSPEED. The calculation of these velocities depends on the values of the average thermal conductivities in the different directions computed in the subroutine THK. Then SUBVOL evaluates the volume of the resistive zone inside each section between two adjacent voltage taps. The knowledge of the normal zone volume and the average value of the resistivity at the actual temperature and field, calculated by the subroutine RHO, makes possible to obtain the resistance of each section and the total resistance of the magnets. The temperature of the normal zone is than computed by solving the heat balance equation and using the subroutines CP and CPMET to have the average specific heat. THK, RHO, CP and CPMET are all linked to a file containing the properties of the different materials in a range of temperature from 4.2 to 300 K.

If a coil is not quenched, all these steps are skipped, the normal zone volume as well as the magnet resistance is set equal to zero, while the temperature inside the winding is set equal to the bath temperature.

When these quantities are obtained for each magnet, the subroutine DCURR solves the electric circuit equations providing the values for the ratio dI/dt for each magnet. Then the voltage at each voltage tap in each coil is calculated as well as the energy dissipated in the winding during the temporal step.

There are several output files providing the values obtained for different quantities; some of them are automatically generated by the program and written by the subroutine SUBWRITE2. For the n–th coil they are:

- **Qn.out** which contains for each time step the values of: time, current, hot spot temperature, resistive volume increment and total voltage across the winding.
- **Qbn.out** which reports the voltage across each section the coil is subdivided by voltage taps.
- **Field$_n$** which contains the magnetic field where it is necessary for quench propagation velocity calculation (cfr 3.2).
- **Vel$_n$.out** where you can find the longitudinal and transversal quench propagation velocity where it is useful for resistive volume evaluation (cfr 3.2) .
- **Thcond$_n$.out** which contains the values for thermal conductivity in longitudinal, radial and axial directions in the same locations where the propagation velocity is required.

Moreover the user can choose to have some additional information by setting in input the parameter *iout*=1 and/or *iwv*=1. If *iout*=1 the following files will be output:

- **Nzdim$_n$.out** containing the normal zone volume and its dimensions in the n–th coil at each temporal step.
- **Res$_n$.out** containing the resistance of each section of the n–th coil at each temporal step.
- **Curr$_n$.out** which reports the current in the magnet, the current flowing in the dumping resistor, the current delivered by the power supply and the value of dI/dt for each temporal step.

If *iwv* is set equal to 1 then the output file **Volum$_n$.out** will be edited for each coil reporting the resistive volumes in each section of the winding.

When all the temporal steps have been executed the subroutine SUBWRITE–3 writes in an output file some information about the state of the coil system at the end of quench evolution like the total energy dissipated in the magnet and what is the maximum voltage and temperature reached.

3 THE CODE DYNQUE: DETAILED DISCUSSION

3.1 Propagation velocity

In order to describe how the normal zone spreads up in a magnet we need to discuss its propagation velocity and, as a coil is a strongly anisotropic medium, different directions are to be taken into account. Let's first consider a single wire: as regards the velocity in longitudinal direction (i.e parallel to the cable and azimuthal in the winding) the normal–superconducting boundary is usually described by a plane thermal wave travelling velocity v_l. An analytical expression for v_l , valid for adiabatic coils and obtained by solving the heat balance equation is given by[1,2]:

$$\begin{cases} v_l = \frac{1}{(\gamma C)}\sqrt{\frac{\rho\lambda_l}{\Theta_m-\Theta_0}} \\ \Theta_m = \frac{\Theta_g+\Theta_0}{2} \end{cases} \qquad (1)$$

Θ_g is the temperature at which ohmic heat generation starts and it is given by:

$$\Theta_g(B,J) = \Theta_c(B,0) - [\Theta_c(B,0) - \Theta_0]\frac{J}{J_{c0}(B)} \qquad (2)$$

$J_{c0}(B)$ is the critical current density at $\Theta = \Theta_0$ and magnetic field B. A linear relationship between J_c and B is assumed at fixed temperature:

$$J_c = mB + q \qquad (3)$$

The value for m and q are obtained by interpolation from experimental data and are required for each cable as input data.

The value for the critical temperature Θ_c at current density J=0 and field B is given by the empirical formula of Lubell[3]:

$$\Theta_c(B) = \Theta_{c0}(1 - \frac{B}{B_0})^{0.55} \quad (4)$$

where:

	Θ_{c0}	B_0
NbTi	9.2 K	14.5 T
Nb_3Sn	18.3 K	22.0 T

Let's now consider a solenoidal winding: the heat produced by ohmic dissipation will diffuse through the insulation in transverse direction too, i.e perpendicular to the cable itself. For the quench propagation velocity in the transverse direction, the following expression has been proposed by Wilson[4]:

$$\frac{v_t}{v_l} = \frac{(\gamma C)_{av.met}}{(\gamma C)_{av.}} \times \sqrt{\frac{\lambda_t}{\lambda_l}} \quad (5)$$

where $(\gamma C)_{av}$ is the specific heat averaged over the total cross section while $(\gamma C)_{av.met}$ averaged over the metallic constituents only.

Due to the fact that λ_t is generally different if evaluated in radial direction (i.e along the coil radius) or in the axial one (i.e parallel to the coil axis) the radial and axial quench propagation velocities v_r and v_a will be different too.

3.2 Magnetic field

In order to give a correct evaluation of the quench propagation velocity, it is necessary to know the magnetic field inside each coil, since Θ_m , λ_l , λ_t depends on field. In order to obtain a field map for every winding at each temporal step we use the following approach. Let's consider N concentric solenoids in a cylindric coordinate system r,ϕ,z, with the z axis coincident with the coils axis and the plane z=0 coincident with the symmetry plane of each winding: the magnetic field $Btot_k$ at radius r and height z of the k–th solenoid will be given for any angle by:

$$Btot_k = B_k(r, z, I_k) + \sum_{i=k+1}^{N} B_{0i}(I_i) \quad (6)$$

where

$B_k(r, z, I_k)$ is the self field generated by the k-th coil at the request point P(r,z) at the current value I_k ;

$B_{0i}(I_i)$ is the magnetic field produced by the i–th winding inside its bore at the current I_i.

In the formula (6) the windings are to be considered numbered from the inner one to the outer one; so in the right–end side the second term represents the contribution to the field from the magnets outside the k–th one. The basic assumption of (6) is to neglect the stray field of every (solenoidal) coil and consider the field generated inside the bore as uniform. Of course this last is not true but very often a coil inserted in a bigger one is usually well shorter, such that the field generated by the external coil onto the internal one does not vary very much (at least at the level of accuracy needed for material properties).

The following values are required for each magnet by Dynque as input for the magnetic field evaluation:

$B_{0i}(I_{0i})$ that is magnetic field produced by the i–th coil at $P(0,0)$ at the initial current value I_{0i};

$B_{Rin}(I_{0i})$ that is magnetic field produced by the i–th coil at $P(Rin_i,0)$ at the initial current value I_{0i};

$B_{hi}(I_{0i})$ that is magnetic field produced by the i–th coil at $P(Rin_i,\frac{H_i}{2})$ at the initial current value I_{0i};

$B_{Rout}(I_{0i})$ that is magnetic field produced by the i–th at $P(Rout_i,0)$ at the initial current value I_{0i}.

At any time the magnetic field in each request point of the k–th coil is obtained assuming:

- A linear dependence of the magnetic field on the current. This means that values for the field B at the initial time are scaled with current at each temporal step.
- $B_{Rout}(I_k)$ constant at $r = Rout_k$ for each z values;
- The magnetic field linearly decreasing with radius;
- The magnetic field linearly and symmetrically decreasing with height from $z = 0$ to $z = \frac{Hm_k}{2}$ and from $z = 0$ to $z = -\frac{Hm_k}{2}$

The magnetic field value in a point P(Rq,Zq) of fig.2 will be obtained from:

$$B(Rq,0) = \frac{B(Rout,0) - B(Rin,0)}{Rout - Rin} \times Rq$$

$$B(Rq,\frac{Hm}{2}) = \frac{B(Rout,\frac{Hm}{2}) - B(Rin,\frac{Hm}{2})}{Rout - Rin} \times Rq$$

$$B(Rq,Zq) = \frac{B(Rq,\frac{Hm}{2}) - B(Rq,0)}{\frac{Hm}{2}} \times Zq$$

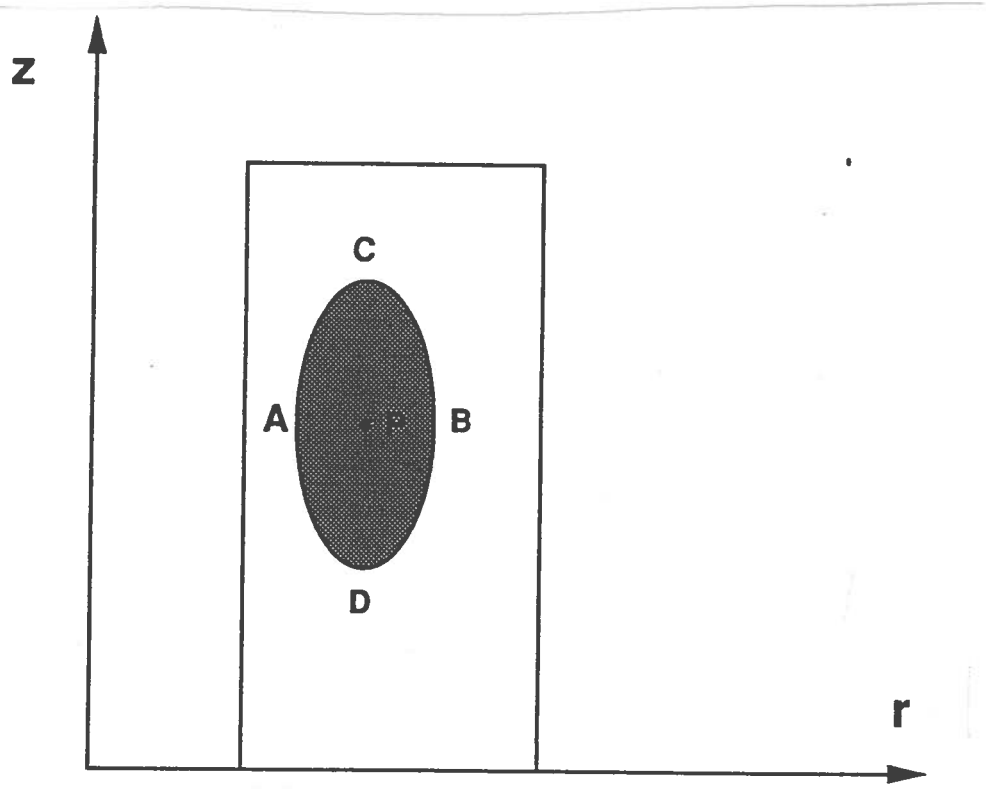

FIG. 2: Normal zone in the plane $\phi = 0$

If a quench starts from the point P(Rq,Zq) at time t=0 inside the k-th coil the normal zone spreads out during the first temporal step with velocities:

$$v_l = v_l[B(Rq, Zq)] = v_l(Rq, Zq) \quad (7)$$

$$v_r = v_l(Rq, Zq) \times \sqrt{\frac{\lambda_r(Rq, Zq)}{\lambda_l(Rq, Zq)}} \quad (8)$$

$$v_a = v_l(Rq, Zq) \times \sqrt{\frac{\lambda_a(Rq, Zq)}{\lambda_l(Rq, Zq)}} \quad (9)$$

Referring to fig.2, at the second temporal step, the field is to be evaluated not only in P but also in:

$A = (r_a, Zq) \quad r_a = Rq - v_r(t_0) \times dt$

$B = (r_b, Zq) \quad r_b = Rq + v_r(t_0) \times dt$

$C = (Rq, z_c) \quad z_c = Zq + v_a(t_0) \times dt$

$D = (Rq, z_d) \quad z_d = Zq - v_a(t_0) \times dt$

and the normal zone will propagate in radial and axial direction no longer symmetrically just because of the different values of the magnetic field in different points. In fact in A, for example, it is:

$$v_{l(A)} = v_l[B(r_a, Zq)] \quad (10)$$

$$v_{r(A)} = v_{l(A)} \times \sqrt{\frac{\lambda_l(r_a, Z_q)}{\lambda_r(r_a, Z_q)}} \quad (11)$$

$$v_{a(A)} = v_{l(A)} \times \sqrt{\frac{\lambda_l(r_a, Z_q)}{\lambda_r(r_a, Z_q)}} \quad (12)$$

while the corresponding values for the quench propagation in B are certainly different because the magnetic field in B is less than in A.

In the program the coordinates of A,B,C,D are evaluated at each temporal step being for the n–th:

$$r_a = R_q - \sum_{i=0}^{n-1} v_{r(A)}(t_i) \times dt$$

$$r_b = R_q + \sum_{i=0}^{n-1} v_{r(B)}(t_i) \times dt$$

$$z_c = Z_q + \sum_{i=0}^{n-1} v_{a(C)}(t_i) \times dt$$

$$z_d = Z_q - \sum_{i=0}^{n-1} v_{a(D)}(t_i) \times dt$$

The magnetic field is then evaluated according to the actual current flowing in each coil and the values for v_l, v_r and v_a are obtained.

3.3 Material properties

Both in (1) and in (5) the specific heat, the thermal conductivity and the resistivity must be averaged over the different constituents of the winding. For this reason the dimensions of the unit cell and the percentage of the materials in it are required as input data by the program. The unit cell is assumed to be rectangularly shaped with a metallic core equivalent to the bare cable surrounded by a uniform layer of insulation. The thickness of the insulation includes both the cable covering (usually glass or varnish) and the resin used for the impregnation.

3.3.1 Thermal conductivity

Regards the transverse and longitudinal thermal conductivity, they can be evaluated considering all the Nc components of the unit cell like thermal conductances in series or in parallel, respectively. In this way in longitudinal direction we'll have:

$$C_l = \sum_{i=1}^{Nc} C_i \quad (13)$$

C_l : effective thermal conductance in longitudinal direction.

C_i : i–th material's thermal conductance.

The formula (13) can be rewritten as:

$$\frac{\lambda_l S}{L} = \sum_{i=1}^{Nc} \frac{\lambda_i S_i}{L} \quad (14)$$

from which:

$$\lambda_l = \sum_{i=1}^{Nc} \lambda_i \frac{S_i}{S}$$

$$\lambda_l = \sum_{i=1}^{Nc} \lambda_i p_i \quad (15)$$

being p_i the percentage in volume of the i-th component in the unitary cell cross section.

As far as the transverse directions are concerned let's first consider the radial one. The unit cell is conceived like three thermal conductances in parallel to each other: the upper and the lower ones in fig.3.a are of insulating material while the central one includes both the metallic core and the insulation on planes parallel to r=constant.

The thermal conductivity in the middle layer is evaluated by assuming this section composed by layers of different materials each one having a surface $S_i = p_i S$ and being, from the thermal point of view, conductances in series to each other.

So the average thermal conductivity in B is calculated from:

$$\frac{1}{C_B} = \sum_{i=1}^{Nc} \frac{1}{C_i} \quad (16)$$

which can be rewritten as:

$$\lambda_B = \frac{L}{\sum \frac{L_i}{\lambda_i}} = \frac{1}{\sum \frac{p'_i}{\lambda_i}} \quad (17)$$

where p'_i is the fraction of the materials inside zone B (see fig.3.a).

Finally, λ_r is obtained from:

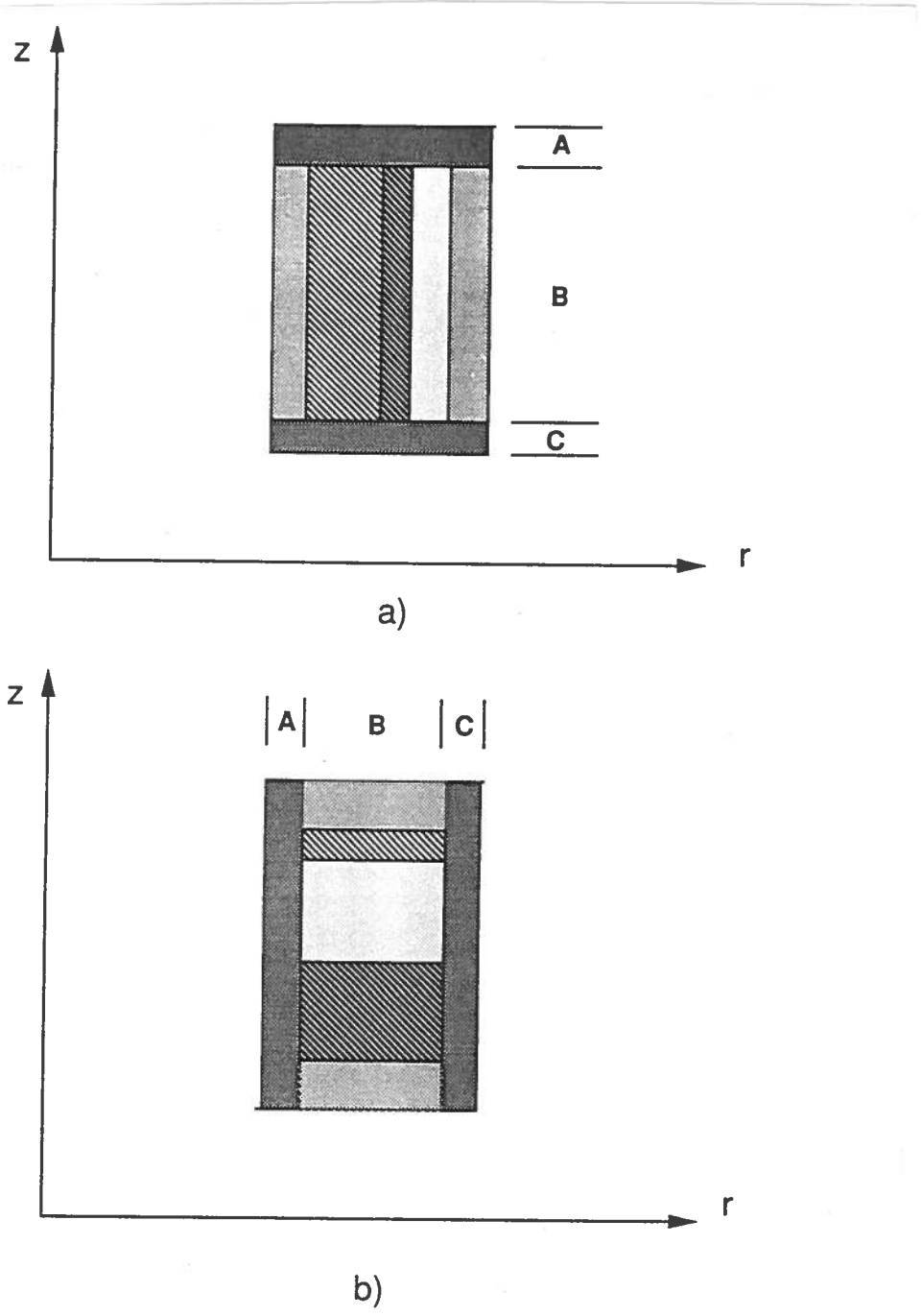

FIG. 3: Unit cell model for thermal conductivity evaluation in radial (a) and axial (b) direction

$$\lambda_r = \lambda_A p_A + \lambda_B p_B + \lambda_C p_C$$

In the same way the thermal conductivity is evaluated in the axial direction, modelling the unit cell area as it is sketched in fig 3.b .

It's worth remarking that, because of the complex structure of the cables and insulation a coil is an highly inhomogeneous and anisotropic medium; for this reason

a right value for λ_l and mainly for λ_t is very hard to reach and their evaluation may be a weak point in the program.

3.3.2 Specific heat

Along the longitudinal direction the heat will propagate mainly through the metallic components, since the insulation of the cable is thermally in parallel and its diffusivity is orders of magnitude less than the cable itself, while heat is forced to propagate also through the insulation in transverse direction. This is why in (5) $(\gamma C)_{av.met}$ is used instead of $(\gamma C)_{av}$.

The specific heat is evaluated at $\Theta = \Theta_m$ whose value depends on current and field; for this reason it is to be calculated at each temporal step. In the program it is possible to choose two different way to take into account the temperature dependence by setting in input *ivel*=1 or *ivel*=2 (i is the $i-th$ temporal step):

1. In the first case it is assumed to be

$$\begin{cases} \gamma C = & (\gamma C)_0 \Theta_i^3 \\ (\gamma C)_0 = & \frac{\gamma C(\Theta_i)|_{t=0}}{\Theta_i^3|_{t=0}} \end{cases} \qquad (18)$$

2. In the second case the mean value of γC in the temperature range $\Theta_0 \leq \Theta \leq \Theta_g$ is calculated:

$$\gamma C = \frac{\int_{\Theta_0}^{\Theta_g} (\gamma C(\Theta))_{av.met} d\Theta}{\Theta_i - \Theta_0} \qquad (19)$$

The values of $\gamma C(\Theta)$, which are used both for expression (19) and in the computation of the temperature increase are obtained by linear interpolation of experimental values from the data base.

3.3.3 Electrical resistivity

The average resistivity per unit volume is computed by assuming the different materials like electrical resistances in parallel each to each other. In this way we'll have:

$$\frac{1}{\rho_{av}(B,\Theta)} = \sum_{i=1}^{Nc} \frac{p_i}{\rho_i(B,\Theta)}$$

and then

$$\rho_{av}(B,\Theta) = 1/\sum_{i=1}^{Nc} \frac{p_i}{\rho_i(B,\Theta)} \qquad (20)$$

How the dependence of ρ from B and Θ are taken into account will be better discussed in section 3.5

3.4 Normal zone volume

Because of the strong anisotropy of the winding, it's very difficult to predict the real shape of the resistive zone at any time. The resistive zone on a section at a fixed angle is in fact quite irregularly shaped, the quench spreading faster where the thermal conductivity and the magnetic field are higher, and slower in those direction where there is an high percentage of insulation or where the magnetic field is weak.

In order to be able to calculate the normal zone volume a simplified model has been taken into account in *Dynque*. Let's first consider the magnetic field be uniform inside the winding: the quench would spread out with velocity v_r towards the coil inner radius and the outer one and with velocity v_a towards the top and the bottom of the coil. In this case we assume that the normal zone envelope at any time t is the surface

$$\begin{cases} \frac{(r-\rho_0)^2}{[R_0(t)]^2} + \frac{(z-\beta)^2}{[Z_0(t)]^2} + \frac{(\phi)^2}{[\phi_0(t)]^2} = 1 \\ Rin \leq r \leq Rout \\ 0 \leq z \leq Hm \end{cases} \qquad (21)$$

where:

r,z,ϕ are the radial,axial and angular coordinates in a cylindrical coordinate system;

P=P(ρ_0, 0, β) is the quench origin;

$R_0(t) = \sum_{k=0}^{I-1} v_r(k) \times dt$ I=actual temporal step, k=index of temporal steps

$Z_0(t) = \sum_{k=0}^{I-1} v_a(k) \times dt$

$\phi_0(t) = \sum_{k=0}^{I-1} \frac{v_l(k) \times dt}{\rho_0}$

The surface (21) satisfies the following conditions:

- At fixed radius r the (21) is an ellipse (fig 4.a) in the angular and axial coordinates with centre $O_1(0,\beta)$ and semi-axes

$$\begin{cases} \phi(r,t) = & \phi_0(t)\alpha(r,t) \\ Z(r,t) = & Z_0(t)\alpha(r,t) \\ \alpha^2(r,t) = & 1 - \frac{(r-\rho_0)^2}{[R_0(t)]^2} \end{cases}$$

- At fixed angle ϕ the (21) is an ellipse (fig 4.b) in the radial and axial coordinates with centre $O_2(\rho_0,\beta)$ and semi-axes

$$\begin{cases} R(\phi,t) = & R_0(t)\sigma(\phi,t) \\ Z(\phi,t) = & Z_0(t)\sigma(\phi,t) \\ \sigma^2(\phi,t) = & 1 - \frac{\phi^2}{[\phi_0(t)]^2} \end{cases}$$

Actually, the field is not uniform inside the coil, as it was previously discussed, so in the real model the normal zone volume is considered to be the sum of 4 quarters of different surfaces like the (21) but with different axes. Let's consider, in fact, the cross

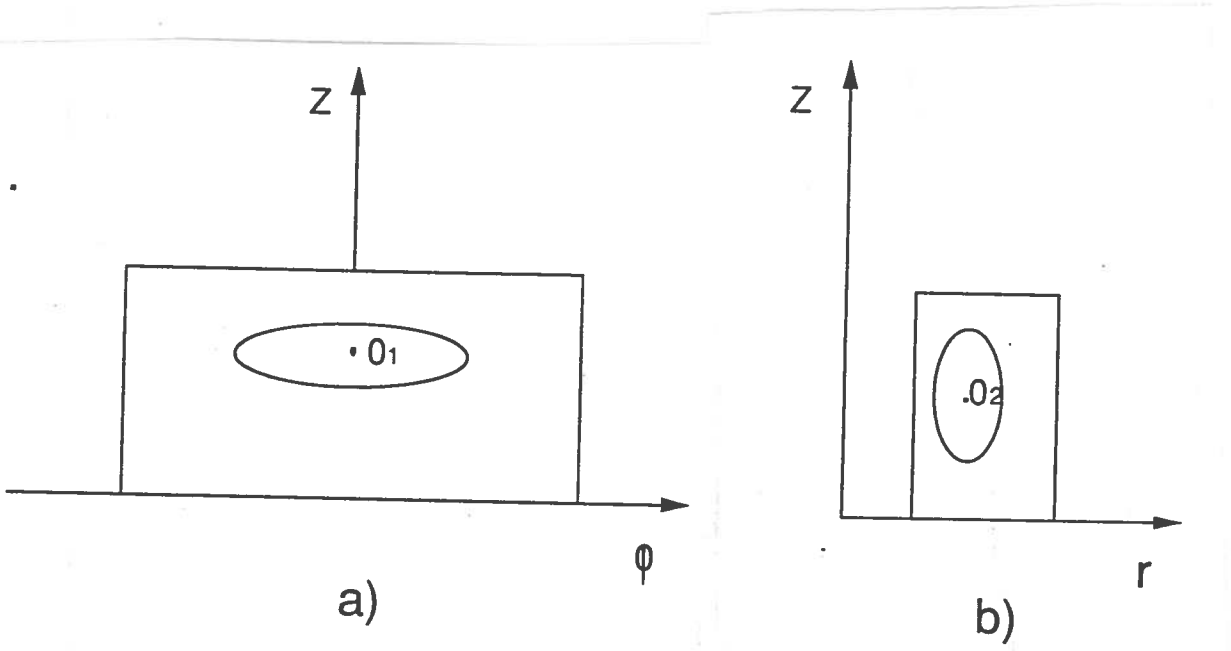

FIG. 4: Normal zone at fixed radius (a) and at a fixed angle (b)

section of the magnet at $\phi = 0$: due to the different value of the magnetic field, the normal zone propagates faster towards the inner radius than towards the outer one so, referring to fig.5(a), $OA > OD$ and for the same reason $OC > OB$.

Being v_{ri} and v_{re} the quench radial velocity towards the internal and the external radius respectively and v_{au} and v_{ad} the axial quench velocity towards the top and the bottom of the coil the ellipse semi–axes are:

$$OB = hu = \sum_{k=0}^{I-1} v_{au}(k) \times dt$$

$$OC = hd = \sum_{k=0}^{I-1} v_{ad}(k) \times dt$$

$$OD = Ri = \sum_{k=0}^{I-1} v_{ri}(k) \times dt$$

$$OA = Re = \sum_{k=0}^{I-1} v_{re}(k) \times dt$$

With this position the code can compute the evolution of a quench started at any point of the winding.

Since each magnet can be supplied with several voltage taps sectioning the coil at different radii, it's very important that the program is able to evaluate not only the total resistive volume inside the coil but also the volume of the quenched zone between two taps. The normal zone calculation is achieved by evaluating at first the area S(r) at

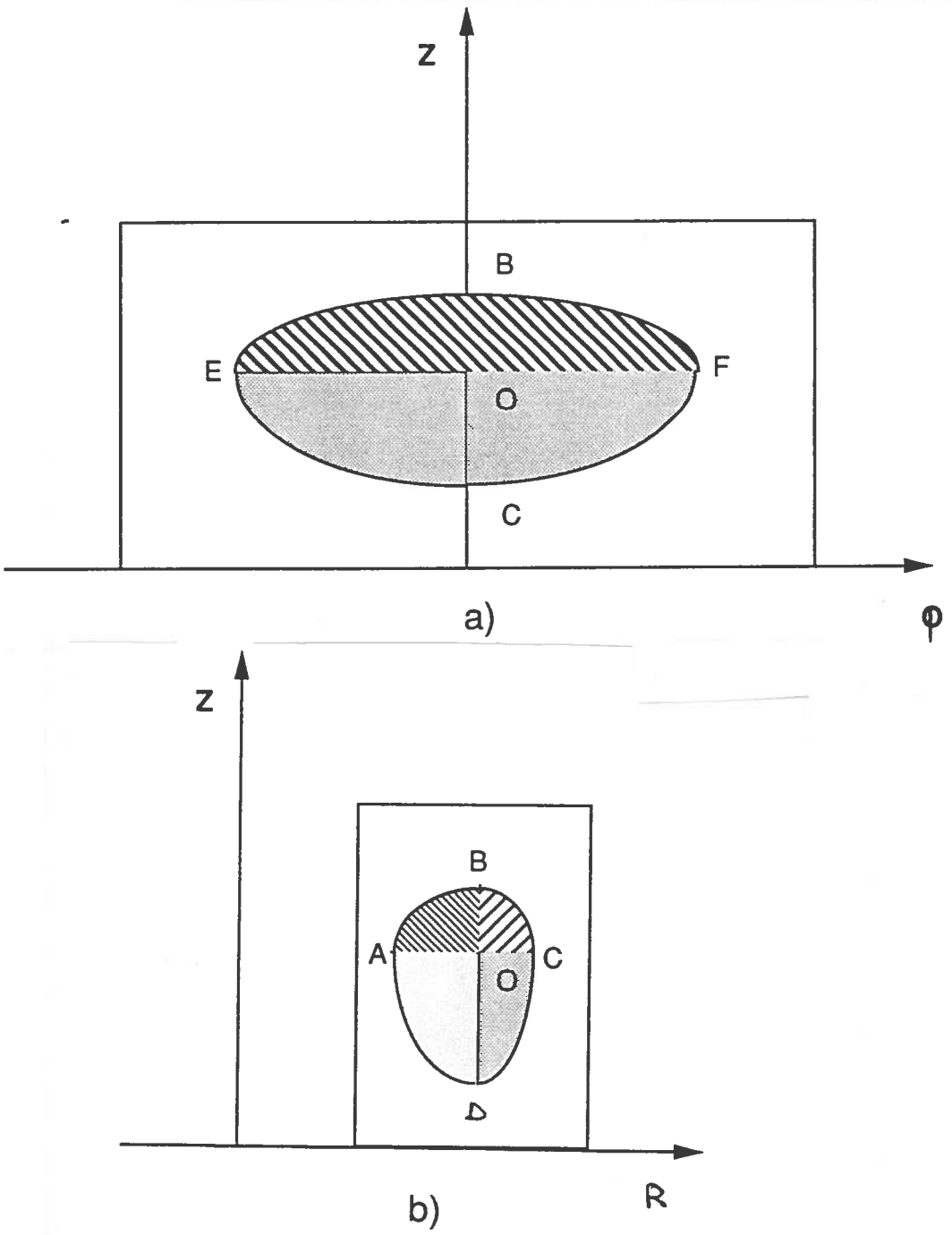

FIG. 5: Asymmetry of the normal zone volume at fixed radius (a) and at fixed angle (b)

a fixed radius r using cylindric coordinates, then the volume for $a \leq r \leq b$ is obtained by integration

$$V = \int_a^b S(r) r dr \quad (22)$$

As it has been remarked S(r) has to be considered as the sum of two half ellipses S(r)=Su(r)+Sd(r) being Su(r) the upper part and Sd(r) the lower area in fig.5.a Several different geometric situations must be taken in account in order to evaluate Su(r). As the same considerations can be done for Sd(r) only the volume for the upper half ellipse

will be worked out.

3.4.1 Case 1: fig 6

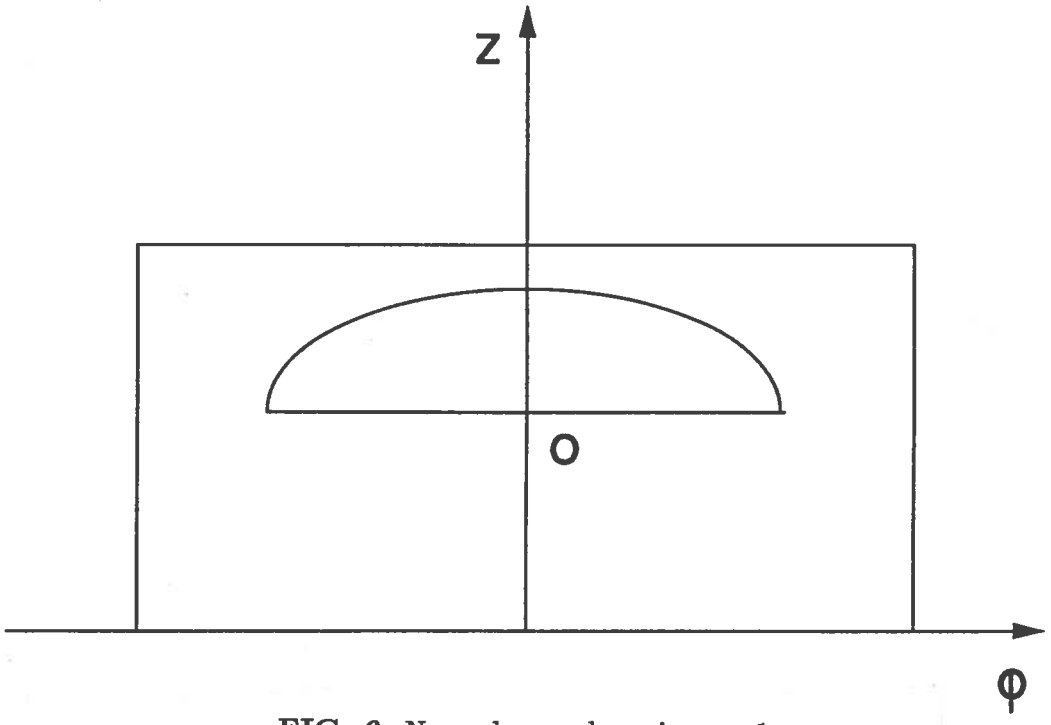

FIG. 6: Normal zone shape in case 1

$$\begin{cases} hu(r) = hu \times \alpha(r) \\ \phi(r) = \phi_0 \alpha(r) \\ hu(r) \leq Hm - \beta \\ \phi(r) \leq \pi \end{cases}$$

In this case it will be:

$$Su(r) = \frac{1}{2}\pi\ hu(r)\ \phi(r) = \frac{1}{2}\pi\ hu\ \alpha(r)\ \phi_0\alpha(r)$$

from which

$$Su(r) = \frac{1}{2}\pi\ hu\ \phi_0\ \alpha^2(r)$$

and the volume for $a \leq r \leq b$

$$V = \frac{1}{2}\int_a^b Su(r) r dr$$

$$V = \frac{\pi Z_0 \phi_0}{2R^2}\left[(R^2 - \rho_0^2)\frac{r^2}{2} + \frac{2}{3}\rho_0 r^3 - \frac{1}{4}r^4\right]_a^b \qquad (23)$$

It has to be remarked that R=Ri if $Rin \leq a \leq r \leq b \leq \rho_0$ while R=Re if $\rho_0 \leq a \leq r \leq b \leq Rout$; this fact will be hereafter implied.

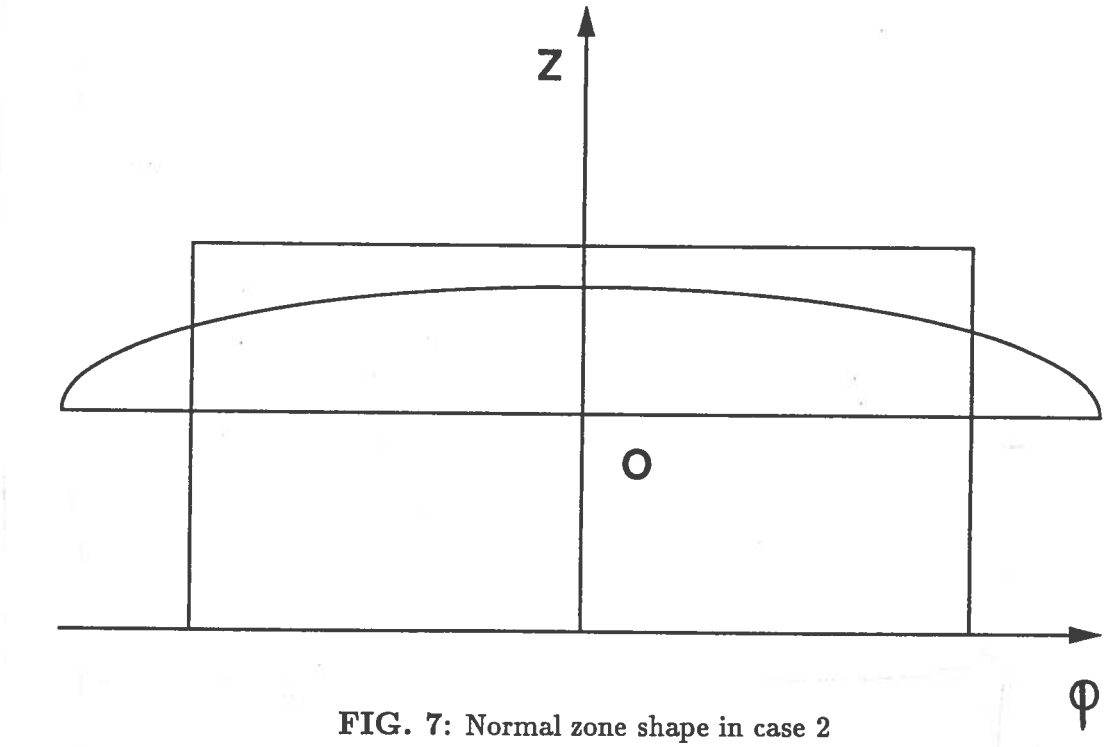

FIG. 7: Normal zone shape in case 2

3.4.2 Case 2: fig.7

$$\begin{cases} hu(r) = hu \times \alpha(r) \\ \phi(r) = \phi_0 \alpha(r) \\ hu(r) \leq Hm - \beta \\ \phi(r) > \pi \end{cases}$$

Setting $\xi = z - \beta$: the equation for the ellipse at fixed r is,

$$\frac{\xi^2}{[Z_0 \alpha(r)]^2} + \frac{\phi^2}{[\alpha(r)\phi_0]^2} = 1 \quad (24)$$

from which

$$\xi(\phi) = \mp Z_0 \times \alpha(r) \times \sqrt{1 - \frac{\phi^2}{[\alpha(r)\phi_0]^2}}$$

$$Su(r) = 2 \int_0^{\pi} \xi(\phi) d\phi$$

$$Su(r) = hu\ \phi_0\ \alpha^2(r) \left\{ \frac{\pi}{\alpha(r)\phi_0} \sqrt{1 - \left(\frac{\pi}{\alpha(r)\phi_0} \right)^2} - arcos \left(\frac{\pi}{\alpha(r)\phi_0} \right) + \frac{\pi}{2} \right\} \quad (25)$$

The volume is obtained by numerical integration using the subroutine SIMPS.

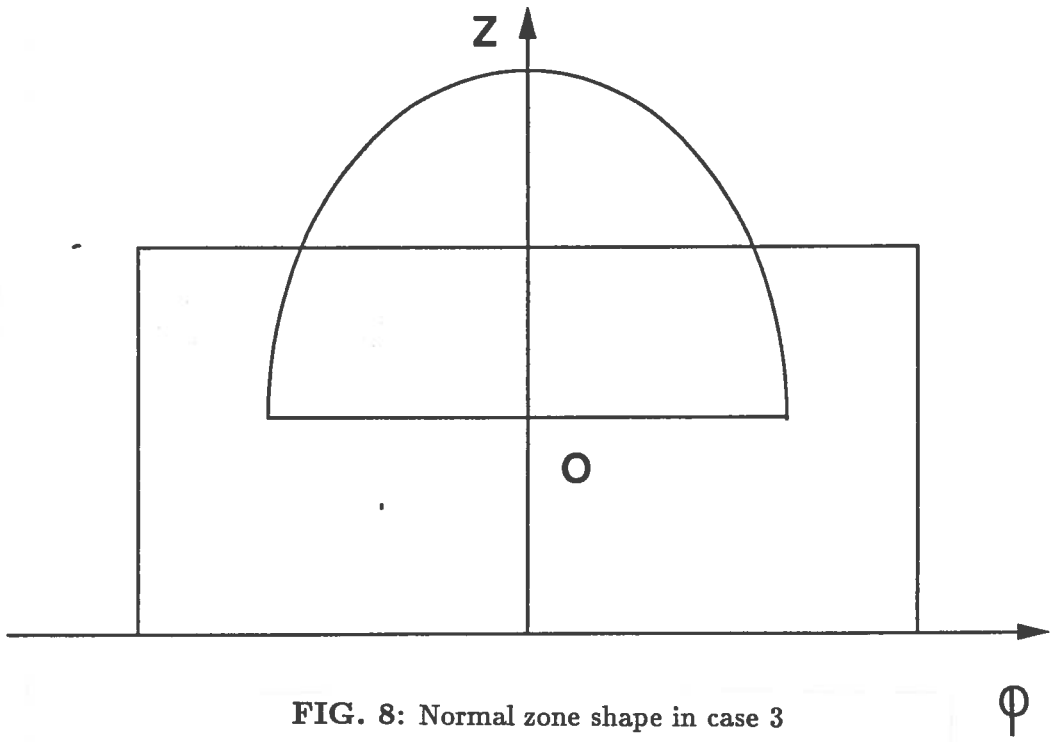

FIG. 8: Normal zone shape in case 3

3.4.3 Case 3: fig.8

$$\begin{cases} hu(r) = hu \times \alpha(r) \\ \phi(r) = \phi_0 \alpha(r) \\ hu(r) > Hm - \beta \\ \phi(r) \leq \pi \end{cases}$$

From the equation (24), which describes the normal zone boundary at fixed radius it is possible to obtain

$$\phi(\xi) = \mp \alpha(r)\phi_0 \sqrt{1 - \left(\frac{\xi}{Z_0 \alpha(r)}\right)^2} \quad (26)$$

The surface Su(r) can then be obtained by integration

$$Su(r) = 2 \int_0^{Hm-\beta} \phi(\xi) d\xi$$

$$\begin{cases} Su(r) = Z_0 \phi_0 \left[K\sqrt{1-K^2} - arcosK + \frac{\pi}{2}\right] \alpha^2(r) \\ K = \frac{Hm-\beta}{Z_0 \alpha(r)} \end{cases} \quad (27)$$

In this case too the volume is obtained by numerical integration using the subroutine SIMPS.

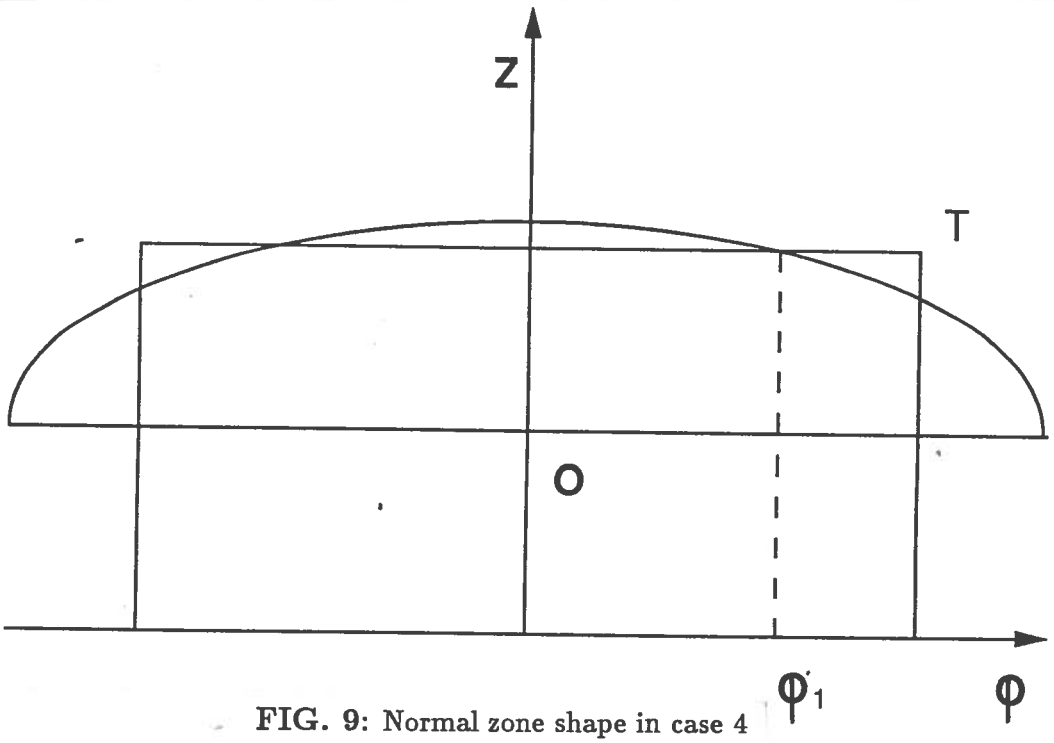

FIG. 9: Normal zone shape in case 4

3.4.4 Case 4: fig.9

Let's now consider the case in which the axes of the ellipse have reached the borders of the coil but there are some superconducting zone left; the normal zone will grow and when the ellipse passes through the point T(π,Hm) the whole magnet will be quenched. For $hu > Hm - \beta$ and $\phi_0 > \pi$ let's find at which value of r the ellipse passes through T.

Replacing in the (21) $\phi = \pi$ and z=Hm we obtain:

$$\frac{(r-\rho_0)^2}{R_0^2} + \frac{Hm-\beta}{Z_0^2} + \frac{\pi}{\phi_0^2} = 1$$

and then

$$r = \rho_0 \mp R_0 \sqrt{1 - \frac{(Hm-\beta)^2}{Z_0^2} - \frac{\pi}{\phi_0^2}} = \rho_0 \mp R_0\sqrt{\Psi}$$

Setting

$$R_{limi} = \rho_0 - R_0\sqrt{\Psi}$$

$$R_{lime} = \rho_0 + R_0\sqrt{\Psi}$$

the situation sketched in fig.9 is described by the conditions:

$$\begin{cases} hu(r) > Hm - \beta \\ \phi(r) > \pi \\ r \leq R_{limi} \ \ or \ \ r \geq R_{lime} \end{cases}$$

Su(r) is obtained from:

$$Su(r) = 2\left[\phi_1 \times (Hm - \beta) + \int_{\phi_1}^{\pi} Z_0\alpha(r)\sqrt{1 - \frac{\phi^2}{[\alpha(r)\phi_0]^2}}d\phi\right] \quad (28)$$

$$\begin{cases} Su(r) = 2\phi_1(Hm - \beta) + Z_0\phi_0\alpha^2(r)\left[\gamma(r)\sqrt{1-\gamma^2} - acos(\gamma(r)) - \delta(r)\sqrt{1-\delta^2(r)} + acos(\delta(r))\right] \\ \gamma(r) = \frac{\pi}{\alpha(r)\phi_0} \\ \delta(r) = \frac{\phi_1}{\alpha(r)\phi_0} \end{cases}$$

3.4.5 Case 5: fig.10

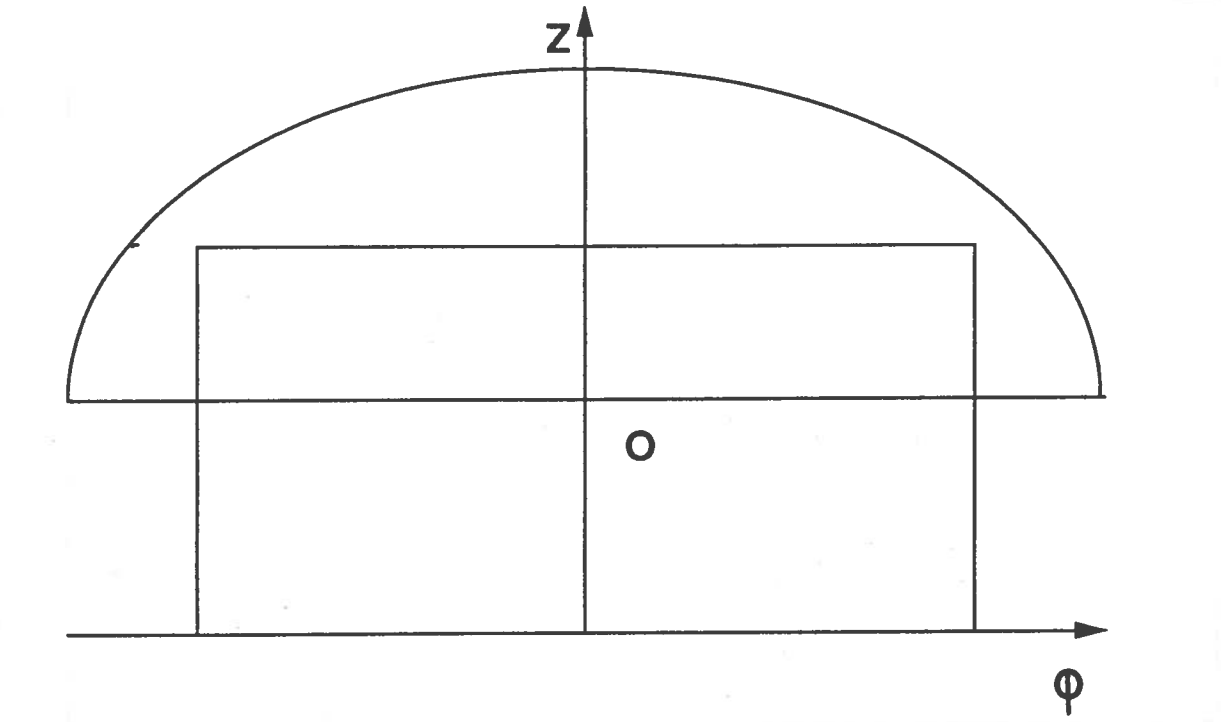

FIG. 10: Normal zone shape in case 5

The last possible situation is when all the superior part of the coil is quenched, that means:

$$\begin{cases} hu(r) > Hm - \beta \\ \phi_0(r) > \pi \\ R_{limi} < r < R_{lime} \end{cases}$$

In this case it's simply:

$$S(r) = 2\pi(Hm - \beta)$$

$$V = \int_a^b 2\pi(Hm - \beta)rdr = \pi(b^2 - a^2)(Hm - \beta) \quad (29)$$

It's important to remark that in integrating in radial dimension inside a zone of the magnet, the shape of S(r) may change from situation 1 to case 5. In order to take this fact in account, the program compares the length of the axes of the ellipses at r=a and r=b with the dimensions of the coil at the same radii and states, in this way, which is S(r) at the borders of the zone taken in account. If S(a) and S(b) have the same shape, the the volume is calculated by a simple integration, otherwise the radii at which it changes are evaluated and the volume is obtained as sum of parts inside of which the shape of S(r) is the same.

3.5 Resistance

When the normal zone volume V is known for each zone the resistance R is obtained by

$$R = \rho(B,T) \times V \quad (30)$$

where ρ is the resistivity per unit volume averaged over the unit cell.

The magnetic field affecting the resistivity of Copper and Aluminum, is assumed to be the average over the total resistive zone:

$$B_{av} = \frac{B_A + B_B + B_C + B_D + B_P}{5} \quad (31)$$

where A, B, C, D, O are the points in fig.5(a).

As far as the temperature is concerned, we must remember that it isn't uniform inside the normal zone. During the first time step dt the normal zone grows up to V_1 and it warms up to $T = T_1^1$ because of ohmic dissipation. During the second time step the resistive zone reaches V_2 so, V_1 has been heated for $2 \times dt$ up to T_2^2 while $V_2 - V_1$ has been heated only for dt up to the temperature T_1^2. In this way, the normal zone at the N–th temporal step is conceived like N concentric shell each one at a different temperature T_i^N such as $T_i^N > T_{i+1}^N$ for i=1,N.

The normal zone resistance at the N–th temporal step is so calculated as:

$$R = \sum_{k=1}^{N} \rho(B_{av}^N, T_k^N) \Delta V_k$$

where B_{av}^N is the averaged field from (31) at the N–th time step and ΔV_k is the normal zone volume increment during the k–th time step.

3.6 Temperature

The temperature of each shell is obtained by solving the thermal balance equation under the hypothesis of local adiabaticity, that is:

$$\rho(\Theta)J^2(t)dt = \gamma C(\Theta)d\Theta \quad (32)$$

In the program the following approximation is used:

$$J_n^2(t_{n+1} - t_n) = \int_{\Theta_n}^{\Theta_{n+1}} \frac{\gamma C(\Theta)}{\rho(\Theta)} d\Theta \quad (33)$$

where J_n^2, t_n, and Θ_n are respectively the density current, the time and the temperature at the n–th temporal step.

The equation (33) is to be solved for all the n layers, each one is increasing in temperature without heat exchange with the cryogenic bath or the adjacent layers, *adiabatic hypothesis.*

While the current is the same for all the layer of each coil, the integral in the right–hand side of equation (33) is to be evaluated for the each layer, at its own temperature (while the magnetic field for resistivity is averaged over the whole normal zone). An iterative predictor–corrector method was chosen, the predictor is (indicating with i the layer index, i = 1...n):

$$\begin{cases} \Theta_{i,n+1}^{(0)} = \Theta_{i,n} + \frac{\rho(\Theta_{i,n})}{\gamma C(\Theta_{i,n})} J_n^2 \Delta t & i \neq n \\ \Theta_{i,n+1}^{(0)} = \Theta_{i,n} + \frac{1}{2}\frac{\rho(\Theta_{i,n})}{\gamma C(\Theta_{i,n})} J_n^2 \Delta t & i = n \end{cases}$$

and the corrector is:

$$\begin{cases} \Theta_{i,n+1}^{(k)} = \Theta_{i,n} + \frac{\rho(\Theta_{i,m}^{(k)})}{\gamma C(\Theta_{i,m}^{(k)})} J_n^2 \Delta t \\ \Theta_{i,m}^{(k)} = \frac{\Theta_{i,n} + \Theta_{i,n+1}^{(k-1)}}{2} \end{cases} \quad (34)$$

where k = 1...5. At the end of the the fifth cycle the last values of $\Theta_{i,n+1}$ is returned as new temperature of the i-th resistive shell.

3.7 Current equations

The equations for current evaluation depend on the electrical circuit configuration which changes during a quench event. Let's first examine the simple case of one coil and we shall extend later to the case of many coils connected in series finally to the case of many coils with different power supplies and independent dumping resistors.

Let's now discuss the possible electric connection of one coil to the room temperature circuit.

3.7.1 CASE 1: $t < \tau_d \quad , V < V_{Max1}, I = I_0$

Any sort of quench detection system (QDS) doesn't break the current supply off instantaneously but after a delay time τ_d so, for $t_0 \leq t \leq \tau_d$ the power supply provides a

constant current. Actually τ_d is the total time required by the QDS both to recognize the start of a quench and the electronic delay before the circuit starts to open.

Due to the growing of the resistive zone, current begins to share between magnets and the dump resistor and a voltage, which is the sum of a resistive and of an inductive signal, shows at the different voltage taps.

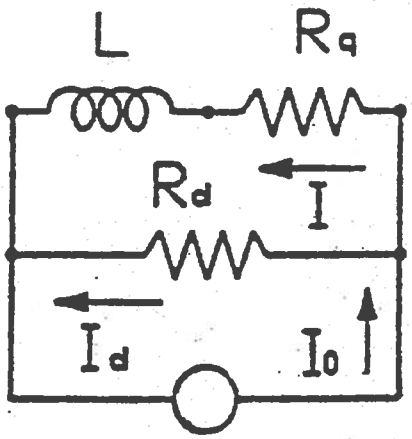

FIG. 11: electric circuit of one quenched coil while still in current mode

During this time the circuit describing one quenched coil will be the one in fig.11 and the equations for the current in the circuit are:

$$\begin{cases} R_q I + L\frac{dI}{dt} - R_d I_d = 0 \\ I_0 = I + I_d \end{cases} \qquad (35)$$

from which we obtain

$$L\frac{dI}{dt} = -(R_d + R_q)I + R_d I_0$$

and then setting $R_T = R_d + R_q$ we have

$$L\frac{dI}{dt} = -R_T I + R_d I_0$$

If we consider Nc coupled coils, each one independently supplied and each one in the configuration of fig.11 the equations for the n–th of them will be:

$$\begin{cases} R_{qn} I_n + \sum_{j=1}^{Nc} M_{n,j}\frac{dI_j}{dt} - R_{dn} I_{dn} = 0 \\ I_{0n} = I_n + I_{dn} \end{cases} \qquad (36)$$

where $M_{n,j}$ is the mutual inductance between the n–th and the j–th coil. The (36) can be rewritten as:

$$\sum_{j=1}^{Nc} M_{n,j}\frac{dI_j}{dt} = -R_{Tn} I_n + R_{dn} I_{0n} \qquad (37)$$

3.7.2 CASE 2: $t < \tau_d$, $V_{Max1} \leq V < V_{Max2}$

Before the opening of the circuit occurs, it may happen that the total voltage across the coil exceeds the maximum value V_{Max2} which the power supply can deliver. In this case, the current supply will switch from current to voltage mode. As a matter of fact, no real power supply can reach the maximum voltage V_{Max2} and suddenly switch to voltage mode: actually at a voltage $V_{Max1} = V_{Max1}(I_0) < V_{Max2}$ the delivered current starts decreasing and the maximum value V_{max2} is smoothly achieved. It is possible to describe the transition from current to voltage mode as a power supply providing a voltage V=V(t) increasing in time from V_{Max1} to V_{Max2}; in this case the circuit equations are:

$$\begin{cases} R_q I + L\frac{dI}{dt} - R_d I_d = 0 \\ V = V(t) = R_d I_d \end{cases} \qquad (38)$$

from which we obtain:

$$L\frac{dI}{dt} = V(t) - R_q I \quad (39)$$

It's very difficult to predict the real shape of V=V(t), which depends on the type and quality of the power supply, so two different equations have been worked out from comparing simulations and experimental data. The user can choose the one he wants to use by setting in input the parameter *ivt* equal to 1 or 2.

In the first case V(t) is assumed to be:

$$V(t) = A\exp(-\frac{(\tau_V - t)^2}{K}) \quad (40)$$

τ_V is the time at which the voltage V_{Max2} is reached and its value must be input like the values for V_{Max1} and V_{Max2} while A and K are obtained by imposing the following conditions:

- Replacing $t = \tau_V$ in the (40) it must be $V(\tau_V) = V_{Max2}$ from which we have:

$$A = V_{Max2}$$

- If t_1 is the time at which the voltage is $V = V_{Max1}$ then it has to be:

$$V_{Max1} = V_{Max2}\exp(-\frac{(\tau_V - t_1)^2}{K})$$

from which we get

$$K = \frac{(\tau_V - t_1)^2}{ln(\frac{V_{Max2}}{V_{Max1}})} \quad (41)$$

The other possible choice for V(t) is:

$$V(t) = A(t - \tau_V)^{2n} + B \quad (42)$$

The values for the parameters A and B are obtained by imposing the same conditions as the in previous case that is $V(t_1) = V_{Max1}$ and $V(\tau_V) = V_{Max2}$. In this way we obtain:

$$V(t) = \left[\frac{V_{Max1} - V_{Max2}}{(t_1 - \tau_V)^{2n}}\right](t - \tau_V)^{2n} + V_{Max2} \quad (43)$$

The values for V_{Max1}, V_{Max2}, and n must be input by the user.

In the more general case of Nc coupled coils the (39) is replaced for the n–th magnet by:

$$\sum_{j=1}^{Nc} M_{n,j}\frac{dI_j}{dt} = V_n(t) - R_{qn}I_n \quad (44)$$

It is important to underline that if $V_{Max1} = V_{Max2}$ the transition of the power supply from current mode to voltage is sharp. In such a case the variable τ_V is not used anymore and the program steps from case 1 to case 3.

3.7.3 CASE 3: $t < \tau_d$, $V \geq V_{Max2}$

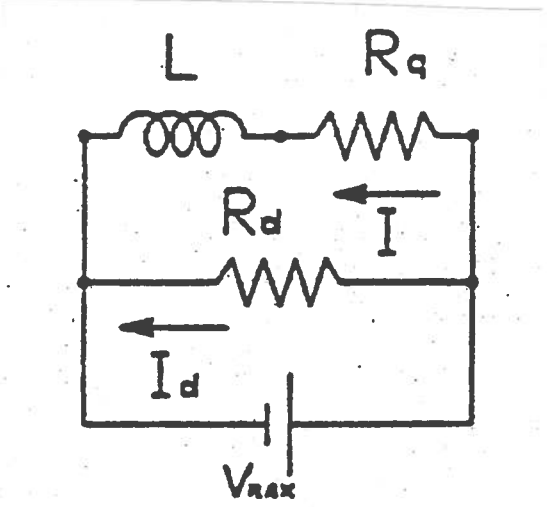

FIG. 12: quenched coil supplied in voltage mode

If the maximum voltage V_{Max2} has been reached and the power supply is not yet off, that is $t \leq \tau_{del}$ the circuit is like the one in fig.12 and the equations for the current are:

$$\begin{cases} R_q I + L\frac{dI}{dt} - R_d I_d = 0 \\ V_{Max2} = R_d I_d \end{cases} \quad (45)$$

from which

$$L\frac{dI}{dt} = V_{Max2} - R_q I \quad (46)$$

or, for the n–th of Nc coupled coils

$$\sum_{j=1}^{N} M_{n,j}\frac{dI_j}{dt} = V_{Max2_n} - R_{qn} I_n \quad (47)$$

3.7.4 CASE 4: $\tau_d \leq t < \tau_d + \tau_{arc}$

When the switch activated by the QDS opens the circuit the current doesn't go down abruptly to zero but flows through an arc for a time τ_{arc} until the arc itself is extinguished. It is possible to schematize with a power supply providing a current $I_0(t)$ decreasing from $I_0(\tau_d)$ to zero in the time τ_{arc}. The circuit describing this situation is the same as fig.11 and the following equations hold:

$$\begin{cases} R_q I + L\frac{dI}{dt} - R_d I_d = 0 \\ I_0(t) = I + I_d \end{cases} \quad (48)$$

As it was previously discussed for V(t) in the situation 2, the time dependence of $I_0(t)$ is not known a priori. Again we use a dependence on time which,among the ones we tested, fits well our experimental data :

$$I_0(t) = I_0 \cos^2\left(\frac{t-\tau_d}{\tau_{arc}}\frac{\pi}{2}\right)$$

From the (48) we obtain:

$$L\frac{dI}{dt} = -R_T I + R_d I_0(\tau_d)\cos^2\left(\frac{t-\tau_d}{\tau_{arc}}\frac{\pi}{2}\right) \quad (49)$$

and for the general case of Nc coupled coils:

$$\sum_{j=1}^{Nc} M_{n,j}\frac{dI_j}{dt} = -R_{T_n} I_n + R_{d_n} I_{0_n}(\tau_{d_n})\cos^2\left(\frac{t-\tau_{d_n}}{\tau_{arc(n)}}\frac{\pi}{2}\right) \quad (50)$$

3.7.5 CASE 5: $t \geq \tau_d + \tau_{arc}$

At the end when the power supply is definitively off we'll have the simple R–L circuit sketched in fig.13 and described by the

$$\begin{cases} R_q I + L\frac{dI}{dt} - R_d I_d = 0 \\ 0 = I + I_d \end{cases} \quad (51)$$

from which we have

$$L\frac{dI}{dt} = -R_T I \quad (52)$$

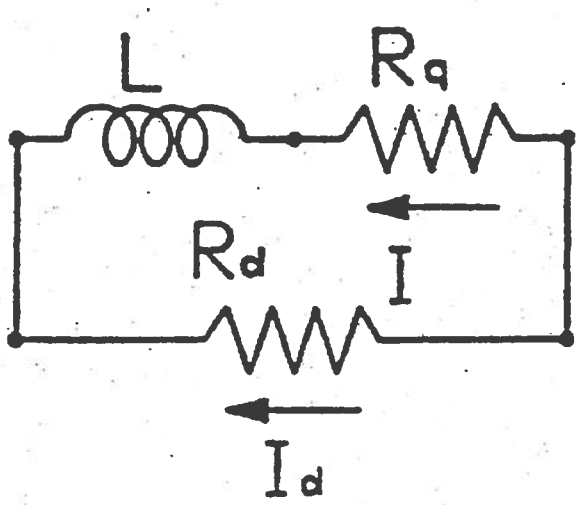

FIG. 13: electric circuit after the power supply has been disconnected

and for the n–th of Nc coupled windings

$$\sum_{j=1}^{Nc} M_{n,j}\frac{dI_j}{dt} = -R_{T_n}I_n \quad (53)$$

Let's now consider Nc coupled coils each one independently supplied: the whole system is described by Nc coupled equations which can be written in matrix form as:

$$\underline{\underline{M}}\,\underline{\dot{I}} = \underline{VETT} \quad (54)$$

where it may be

$VETT(n) = -R_{T_n}I_n + R_{d_n}I_{0_n}$

$VETT(n) = V_n(t) - R_{q_n}I_n$

$VETT(n) = V_{Max2_n} - R_{q_n}I_n$

$VETT(n) = -R_{T_n}I_n + R_{d_n}I_{0_n}\cos^2(\frac{t-\tau_{d(n)}}{\tau_{arc}}\frac{\pi}{2})$

$VETT(n) = -R_{T_n}I_n$

depending on the state of the n–th coil at the considered time.

At last, in order to be able to simulate the quench effects in a quite general situation we have to describe what are the equations to be used when some magnets are connected in series each other. Let's so consider the circuit in fig.14 where there are two coils in series to each other and in parallel with a dump resistor R_d.

The first equation of (38) in this case is:

$$(L_1 + L_2 + 2M_{1,2})\frac{dI}{dt} + (R_1 + R_2)I = R_dI_d$$

If there were Ns coils connected in series, we would have:

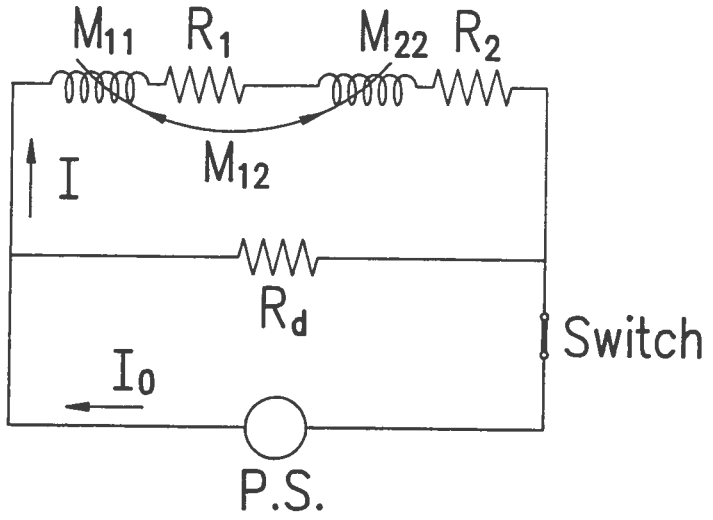

FIG. 14: electric circuit when two coils are series supplied

$$(\sum_{i,j} M_{i,j})\frac{dI}{dt} + (\sum_{k=1}^{Ns} R_k)I = R_d I_d$$

So we can say that a circuit of Ns coils all connected in series is equivalent to a circuit with only one magnet whose inductance and resistance respectively are:

$$\mathcal{L} = \sum_{i,j} M_{i,j}$$

$$\mathcal{R} = \sum_{k=1}^{Ns} R_k$$

In this way the (54) can still be used only replacing L with $\mathcal{L}$ and R with $\mathcal{R}$.

In a more general case we may have several coils, some of which connected in series and with one dumping resistor in parallel, others independently supplied but all magnetically coupled.

In order to give a simple example of this situation let's consider the circuit in fig.15 which describes the magnet *SOLEMI-1 + SOLEMI-2* from the electrical point of view: it is

$$\begin{cases} (M_{1,1} + M_{2,2} + 2M_{1,2})\frac{dI_1}{dt} + (R_1 + R_2)I_1 + (M_{1,3} + M_{1,4} + M_{2,3} + M_{2,4})\frac{dI_2}{dt} = R_{d1}I_{d1} \\ (M_{3,3} + M_{4,4} + 2M_{3,4})\frac{dI_2}{dt} + (R_3 + R_4)I_2 + (M_{3,1} + M_{3,2} + M_{4,1} + M_{4,2})\frac{dI_1}{dt} = R_{d2}I_{d2} \end{cases}$$

Setting:

$\mathcal{M}_1 = M_{1,1} + M_{1,2} + M_{2,1} + M_{2,2}$

$\mathcal{M}_2 = M_{3,3} + M_{3,4} + M_{4,3} + M_{4,4}$

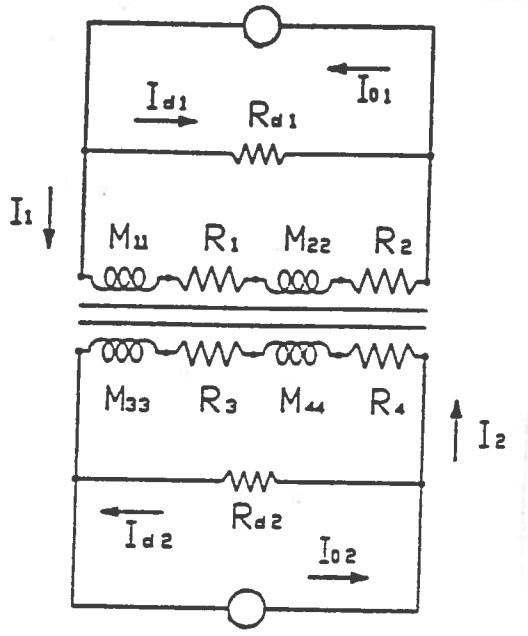

FIG. 15: electric circuit of the *SOLEMI* facility

$\mathcal{M}_{1,2} = \mathcal{M}_{2,1} = M_{1,3} + M_{1,4} + M_{2,3} + M_{2,4}$
$\mathcal{R}_1 = R_1 + R_2$
$\mathcal{R}_2 = R_3 + R_4$

the system can by described by the following equations as two coils independently supplied and magnetically coupled

$$\begin{bmatrix} \mathcal{M}_1 & \mathcal{M}_{1,2} \\ \mathcal{M}_{2,1} & \mathcal{M}_{2,2} \end{bmatrix} \begin{bmatrix} \frac{dI_1}{dt} \\ \frac{dI_2}{dt} \end{bmatrix} + \begin{bmatrix} \mathcal{R}_1 I_1 \\ \mathcal{R}_2 I_2 \end{bmatrix} = \begin{bmatrix} R_{d1} I_{d1} \\ R_{d2} I_{d2} \end{bmatrix} \quad (55)$$

We can think to obtain $\mathcal{M}_i$ writing the inductance matrix of the complete system, subdividing it into blocks as shown below and adding the terms belonging to the same block.

$$\begin{bmatrix} M_{1,1} & M_{1,2} & M_{1,3} & M_{1,4} \\ M_{2,1} & M_{2,2} & M_{2,3} & M_{2,4} \\ M_{3,1} & M_{3,2} & M_{3,3} & M_{3,4} \\ M_{4,1} & M_{4,2} & M_{4,3} & M_{4,4} \end{bmatrix} = \begin{bmatrix} \mathcal{M}_1 & \mathcal{M}_{1,2} \\ \mathcal{M}_{2,1} & \mathcal{M}_{2,2} \end{bmatrix} \quad (56)$$

Both the matrix at the left–hand of the (56) and the one on the right–hand side are required by *Dynque* in input.

Solving the circuit equations, the value $\frac{dI}{dt}$ for each independently supplied system is obtained at time t; then the current at time $t + \Delta t$ is calculated by :

$$I(t + \Delta t) = I(t) + \left.\frac{dI}{dt}\right|_t \times \Delta t$$

3.8 Partial and total voltage calculation

When the current and its time derivative is known for each magnet, it's possible to evaluate the voltages across adjacent taps. These values are the sum of three different terms:

1. The voltage due to the resistance of the normal zone in the section;
2. The voltage due to the mutual inductance between the section taken into account and the others of the same magnet.
3. The voltage due to the mutual inductance between the section and the other coils.

In this way, if we have Nc coils and the n–th of them is subdivided in $\mathcal{N}(n)$ sections, the voltage between the i–th and (i+1)–th voltage taps is:

$$V_{q_i}|_n = R_{i_n} I_n + \sum_{j=1}^{\mathcal{N}(n)} M_{i,j}^{(n)} \frac{dI_n}{dt} + \sum_{k=1,k\neq n}^{Nc} M_{i,k} \frac{dI_k}{dt}$$

and the total voltage across the n–th magnet is obtained by adding:

$$V_n = \sum_{i=1}^{\mathcal{N}(n)} V_{q_i}|_n = \sum_{i=1}^{\mathcal{N}(n)} \left[R_{i_n} I_n + \sum_{j=1}^{\mathcal{N}(n)} M_{i,j}^{(n)} \frac{dI_n}{dt} + \sum_{k=1,k\neq n}^{Nc} M_{i,k} \frac{dI_k}{dt} \right]$$

4 EXPERIMENTAL MEASUREMENTS AND THEIR COMPARISON WITH SIMULATIONS OBTAINED BY DYNQUE.

4.1 Test Magnets

Quench simulations have been compared with experimental data both from *SOLEMI-1* [5] and from two test magnets[6] system wound in our laboratory each one consisting of an outer NbTi coil and an inner one in Nb_3Sn.

SOLEMI-1 is a big fully impregnated NbTi magnet consisting of two coils; each winding is provided with 3 voltage taps and so it is divided into two sections. In table 1 the main characteristics of this magnet are shown. Quenches have been induced at the innermost radius in the middle plane by a heater at different values of current and a quench detection system (QDS) has always been used to detect the quench and automatically switch off the power.

As regards the home made test magnets, their main characteristics are summarized in table 2, while in fig.16 a vertical section of the first magnet, Lasa2–Lasa3, is shown.

Each winding has one section only and $3 \div 5$ voltage taps; any coil can also be independently supplied. Also in this case quenches have been induced at the innermost radius in the middle plane, a QDS has been used sometimes while the switch has been

TABLE 1: Electrical and geometric characteristics of *SOLEMI-1*

	inner coil	*outer coil*
Core size (mm)	1.3×2.9	1.3 ×2.6
No. of strands	13 NbTi/Cu	7 NbTi/Cu + 7 Cu
strands diameter (mm)	0.84	s/c 0.67 + Cu 0.55
cable transposition length (mm)	60	60
cable dimensions (mm)	2.8 ×4.4	2.4 ×3.7
Cu cross section (mm^2)	8.378	6.61
NbTi cross section (mm^2)	2.425	0.889
Cu:NbTi	3.5	7.37
solder cross section (mm^2)	1.5	1.38
total Cu : non Cu	2.13	2.92
RRR (at zero field)	118	≥100
insulation thickness (mm)	0.2	0.2
winding unit cell (mm)	3.2 ×4.8	2.8 ×4.1
cross section (mm^2)	15.36	11.48
requested I_c at 4.2 K	1500 @ 8.7 T	1250 @ 6.5 T
measured cable I_c (A)	1730 @ 8.7 T	1377 @ 6.5 T
NbTi J_c A/mm^2	713	1404
total length (m)	4900 (2 pieces)	16500 (12 pieces)
inner radius (mm)	317	377.4
outer radius (mm)	355.4	455.8
length (mm)	907.2	910.2
layer	12	28
turn number	2266	6227
section inductance (H)	1.82	19.7
total inductance (H)	30.44	
magnet current at 8 T (A)	905	
non copper J_c A/mm^2	715	1550
overall J_c A/mm^2	58.9	78.8
max. voltage to ground (kV)	2	

opened by hand other times. Some measures have been carried on using the coils connected in series and others with the windings independently supplied.

4.2 Procedure and results

All the recorded voltages are the sum of two terms: a positive one due to normal zone resistance and a negative one induced by mutual coupling. By comparing simulations and experimental data detailed information about quench propagation velocities can be gained in particular if the coil is equipped with some intermediate voltage taps.In fact, it's important to point out that the current decay and the total voltage drop

TABLE 2: characteristics of the LASA magnets

NbTi cable	
Wire diameter	0.5 mm
Insulation thickness	0.021 mm
Cu:NbTi	1.35
Nb_3Sn cable	
Wire diameter	0.70 mm
Insulation thickness	0.07 mm
Cu:non Cu	1:4
Magnet Lasa 2 (NbTi)	
Diameter	$\phi_{int} = 45$ $\phi_{ext} = 74$ mm
Height	h = 100 mm
Critical current	$I_c \simeq 135$ (A)
$B_{0_{max}}$	$\simeq 7$ Tesla
Magnet Lasa 3 (Nb_3Sn)	
Diameter	$\phi_{int} = 15.5$ $\phi_{ext} = 39.5$ mm
Height	h = 59.5 mm
Critical current	$I_c \simeq 320$ (A)
$B_{0_{max}}$	$\simeq 6.5$ Tesla
Lasa–2 Lasa–3	
Critical current	$I_c \simeq 135$ (A)
$B_{0_{max}}$	$\simeq 9.7$ Tesla
Magnet Lasa 4 (NbTi)	
Diameter	$\phi_{int} = 92.7$ $\phi_{ext} = 67.8$ mm
Height	h = 201 mm
Critical current	$I_c \simeq 120$ (A)
$B_{0_{max}}$	$\simeq 6.5$ Tesla
Magnet Lasa–5 (Nb_3Sn)	
Diameter	$\phi_{int} = 20.3$ $\phi_{ext} = 62.3$ mm
Height	h = 121 mm
Critical current	$I_c \simeq 220$ (A)
$B_{0_{max}}$	$\simeq 8.5$ Tesla
Lasa–4 Lasa–5	
Critical current	$I_c \simeq 120$ (A)
$B_{0_{max}}$	$\simeq 11$ Tesla

across the winding depend only on the inductance value and on the total resistance of the coil, which changes with time because the volume and temperature are increasing during a quench event. So it's impossible to distinguish the case shown in fig.17(a), where the normal zone propagates faster in axial direction than in radial one, from the case sketched in fig.17(b) where the radial propagation is faster if we can know only the current decay and the total voltage across the magnet. On the contrary if we can

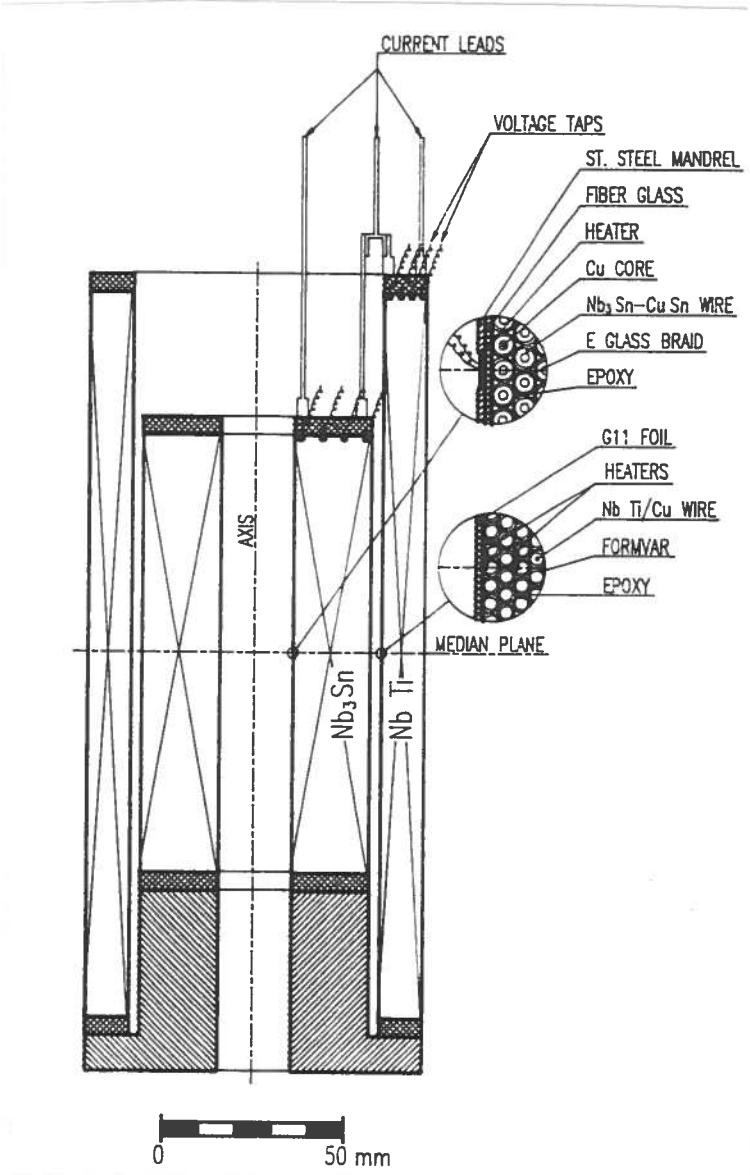

FIG. 16: Vertical section of the magnet Lasa2–Lasa3

measure the voltage drop at each section it is possible to understand which is the real situation and how fast the normal zone spreads in the two transverse directions.

In the computer program the nominal values for v_l, v_r and v_a as given by the (1) and the (5) formulae can be multiplied by correcting coefficients *corvl, corvr, corva* whose value is determined by the best fit of the experimental behaviour.

Using the values reported in table 3 a good agreement between experiments and simulations has been reached:

These values are almost constant and they are the only ones realising a good agreement with experiments.

Let's discuss now few comparison between experiments and simulations. At first the effects of an induced quench at $I_0 = 678A$ $(B = 6T)$ on *SOLEMI-1* will be shown. The quench was induced at the inner coil but after 2s also the outer winding spontaneously

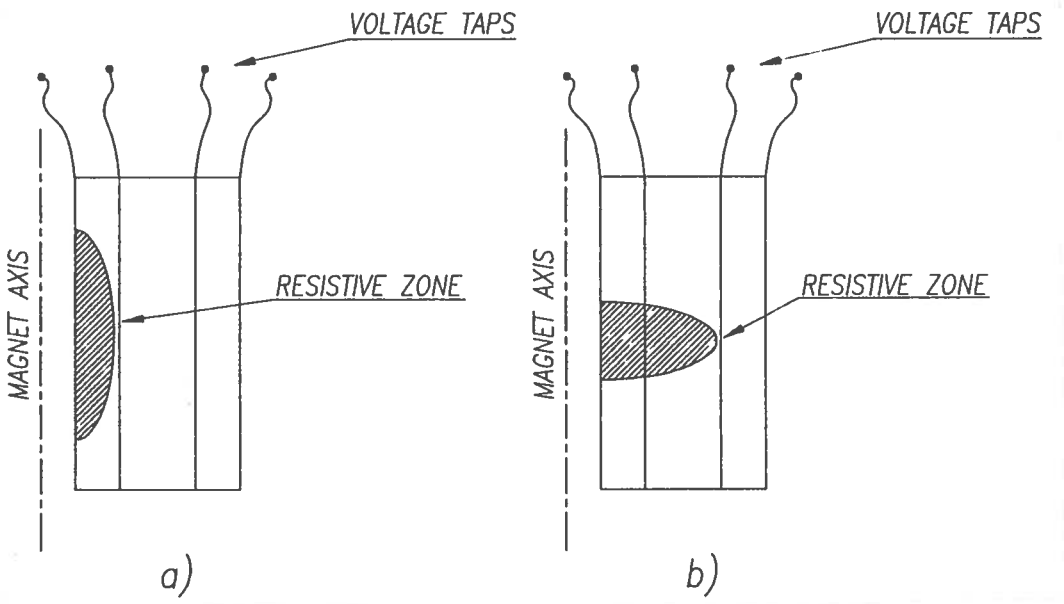

FIG. 17: Utility of intermediate voltage taps in measuring quench propagation velocities in transverse direction

Coil	Material	Corvl	Corvr	Corva
Lasa–2	NbTi	1	$0.22 \div 0.35$	$0.37 \div 0.4$
Lasa–4	NbTi	1	$0.25 \div 0.32$	$0.72 \div 0.74$
Solemi–1	NbTi	1	$0.35 \div 0.41$	$0.49 \div 0.62$
Lasa–3	Nb_3Sn	1	1	0.55
Lasa–5	Nb_3Sn	1	0.95	$0.25 \div 0.4$

quenched, probably due to the sudden flux changing. We measured the voltage across the two sections of the inner coil during the 2s before the power supply switching off which means at a constant current. In this way only the resistive component of the voltage, due to the normal zone was detected. During this time the data were stored at 200 Hz. It takes about 40s for the current to go down to zero after the breaking of the supply and during this time we measured and stored the values of the current and of the voltage across each section with a frequence of 4.6 Hz. We found out the correct values for the correcting parameters by comparing the tracks of the voltage during the first 2s (fig.18) and we used them both for the inner and the outer windings to simulate the system evolution during the following 40s.

As it is shown in fig.19 the agreement is quite good. The same agreement has been found for all the other measurements which have been carried out at different current values.

In fig.20 the current decay and voltages of several sections are shown for the magnet

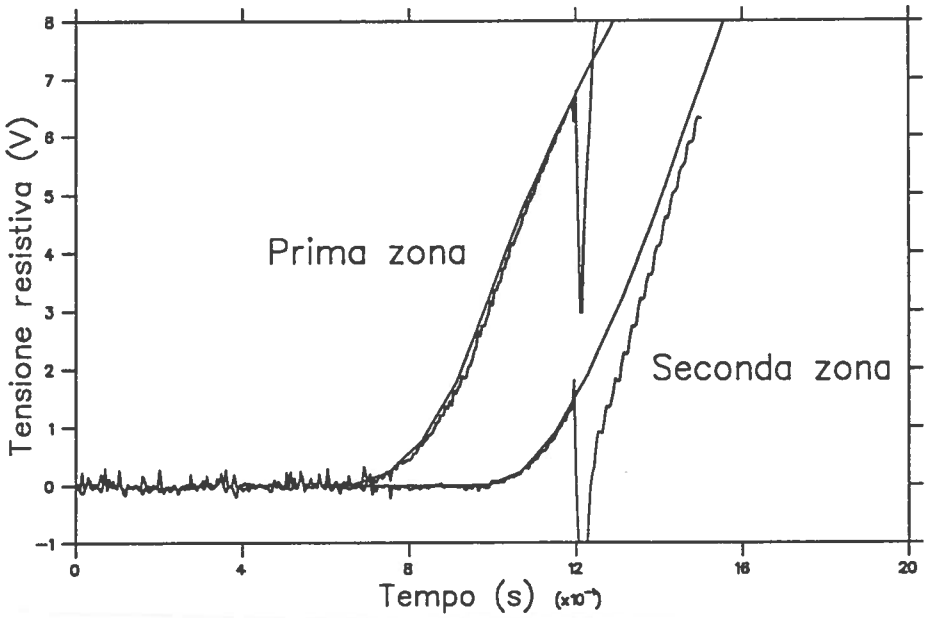

FIG. 18: Comparison between calculated (smooth line) and measured voltage across the two sections of *SOLEMI-1* inner coil after a quench has started. The large negative peaks are due to circuit breaker intervention

Lasa2–Lasa3 when a quench was induced in Lasa2 at $I_0 = 100\,A \;\; B = 7\,T$ while fig.21 shows the experimental results and the simulations for a quench induced at Lasa–5 connected in series with Lasa–4 at $I_0 = 90\,A \;\; B = 8.25T$. In both cases the QDS hasn't been used and the power supply was switched off when the current was already very low. This is why very high positive voltage arisen at the terminals of the quenched coil.

The agreement is quite good also in these examples even if for the Nb_3Sn the fitting between experiments and simulations is not as satisfactory as it is for the NbTi.

5 CONCLUSIONS

A computer program to predict quench behaviour in multicoil and multisection magnets has been developed and tested in our lab. Its agreement with the preliminary measurements seems very good. The analytical formula (1) for the longitudinal velocity of quench propagation has been used and a good agreement between theory and experiments has been found.

The transverse velocities for quench propagation have been obtained from a semi–empirical formula both for NbTi and Nb_3Sn with *ad hoc* coefficients. Changing the formulation for this key velocity is very easy with this code.

Other measurements are going to be carried on in particular on Nb_3Sn and the dependence, if there is one, of the correcting coefficients on the dimensions and on composition of the cable is to be deeper investigated.

The program will be soon implemented to handle magnet working in persistent

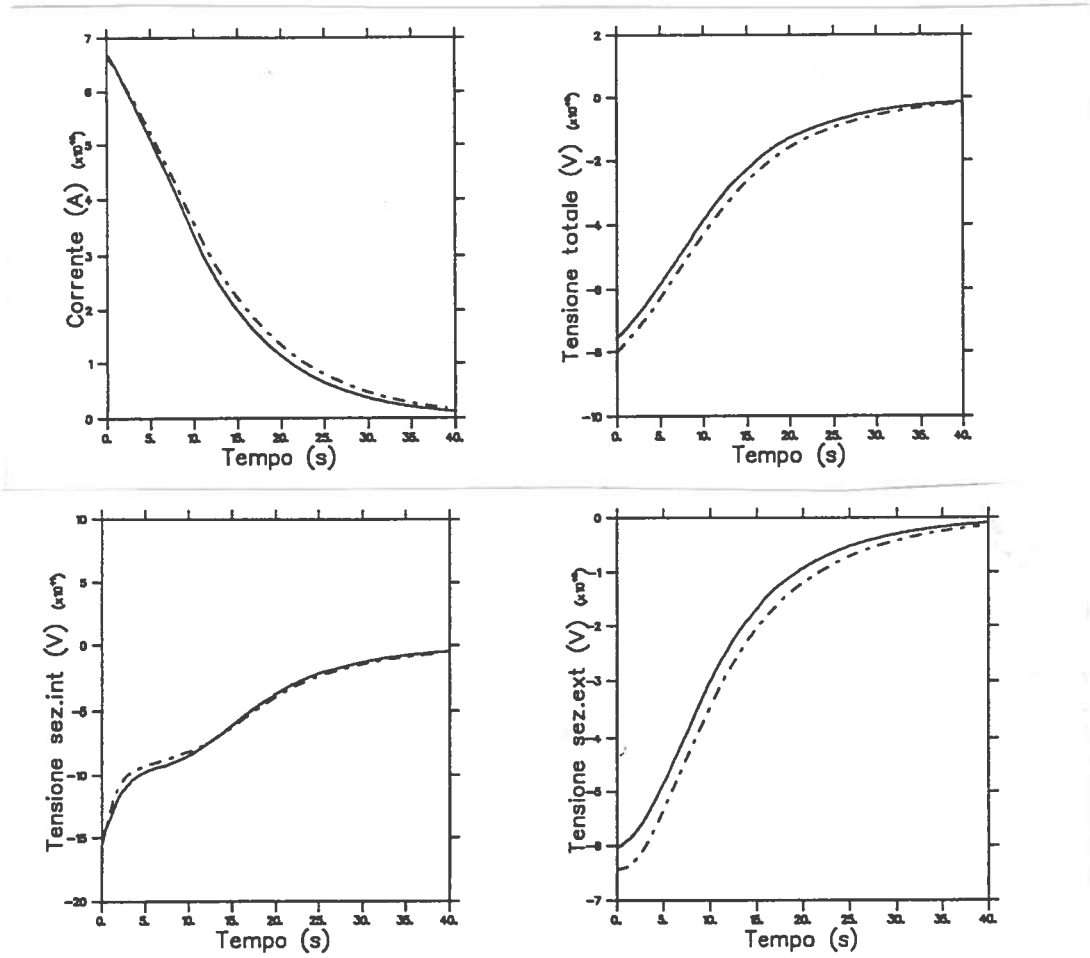

FIG. 19: Current decay and voltage across the whole coil and across the internal and external section during a quench of *SOLEMI-1* at I=678 A and B=6 T. Solid lines: measurements, dashed lines: computer simulation

mode, with shunt resistor in parallel to each winding.

6 ACKNOWLEDGEMENTS

The authors gratefully acknowledge the contribution of Dr. S. Piuri, especially for the calculation of the effective thermal conductivity and the solving method of the temperature equation.

REFERENCES

(1) **W.H.Cherry, J.J.Gittleman,** *Solid state electronics* 1,287 (1960)

(2) **L.Dresner,** *Proc. ASC 1978, IEEE Trans. on Mag.* Mag–15 328 (1979)

(3) **M.S. Lubell,** *Proc. ASC 1982, IEEE Trans. on Mag.* Mag–19, 754 (1983)

(4) **M.N. Wilson,** *Superconducting Magnets*, Clarendon Press Oxford 1983

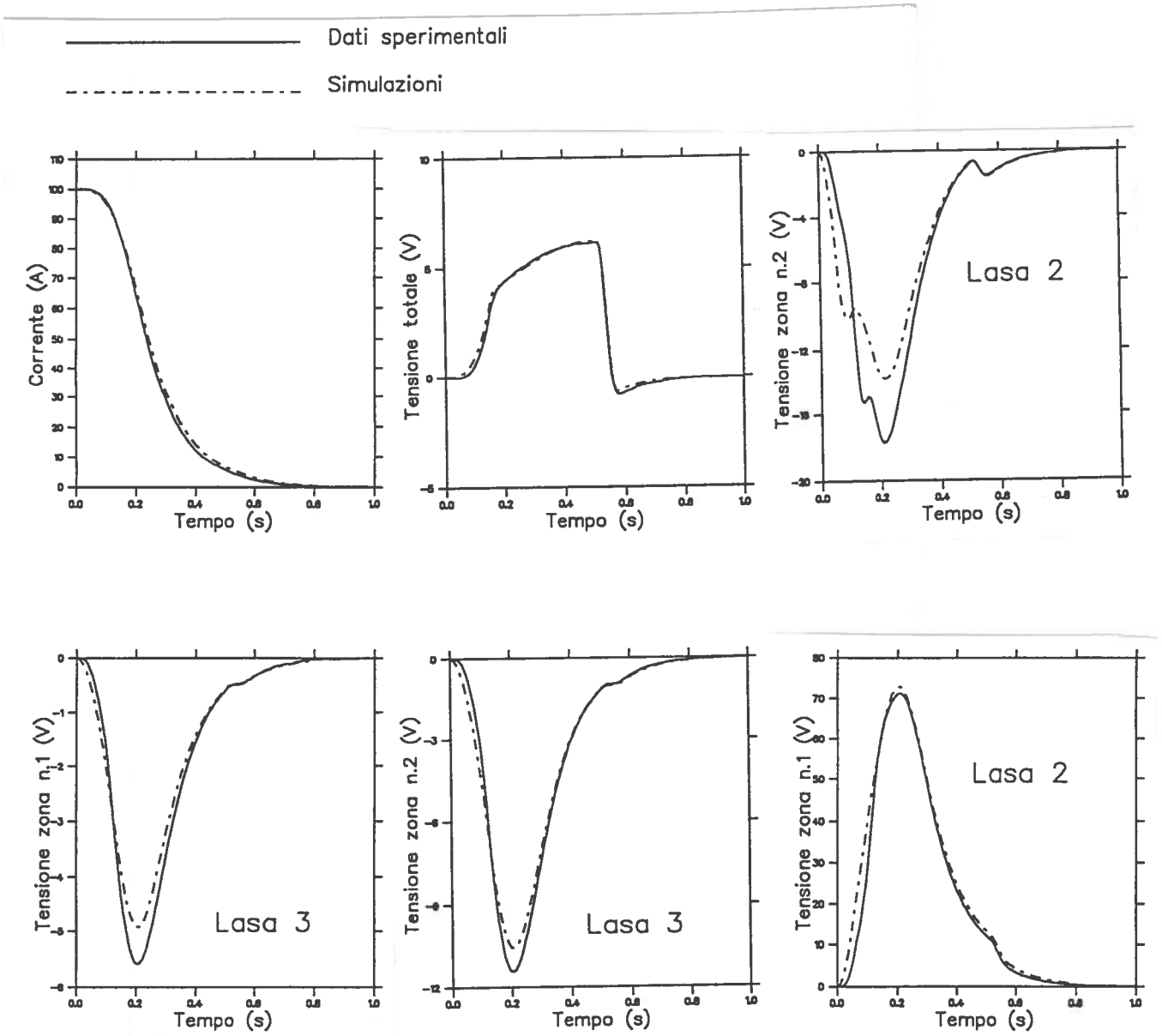

FIG. 20: Measured (solid lines) and computed (dashed) current decay and voltage during a quench of Lasa2–Lasa3 at I=60 A.

(5) **E.Acerbi, G.Baccaglioni, P.Jarvis, J.Mellors, L.Rossi, M.Thoner, G.Volpini,** *The 18 Tesla–100 mm 4.2 K Free Bore Solenoid for LASA–Milan,* IEEE Trans. on Mag. vol.28, N.1, January 1992, p.428

(6) **G.Baccaglioni, M.Canali, G.C.Cartegni, C.Fumagalli, M.Fusetti, L.Gini, L.Grilli, A.Leone,** *Costruzione di solenoidi superconduttori con campo di 10 tesla, presso il laboratorio L.A.S.A, per studi di transizione dallo stato superconduttivo a quello resistivo,* INFN/TC–92/2

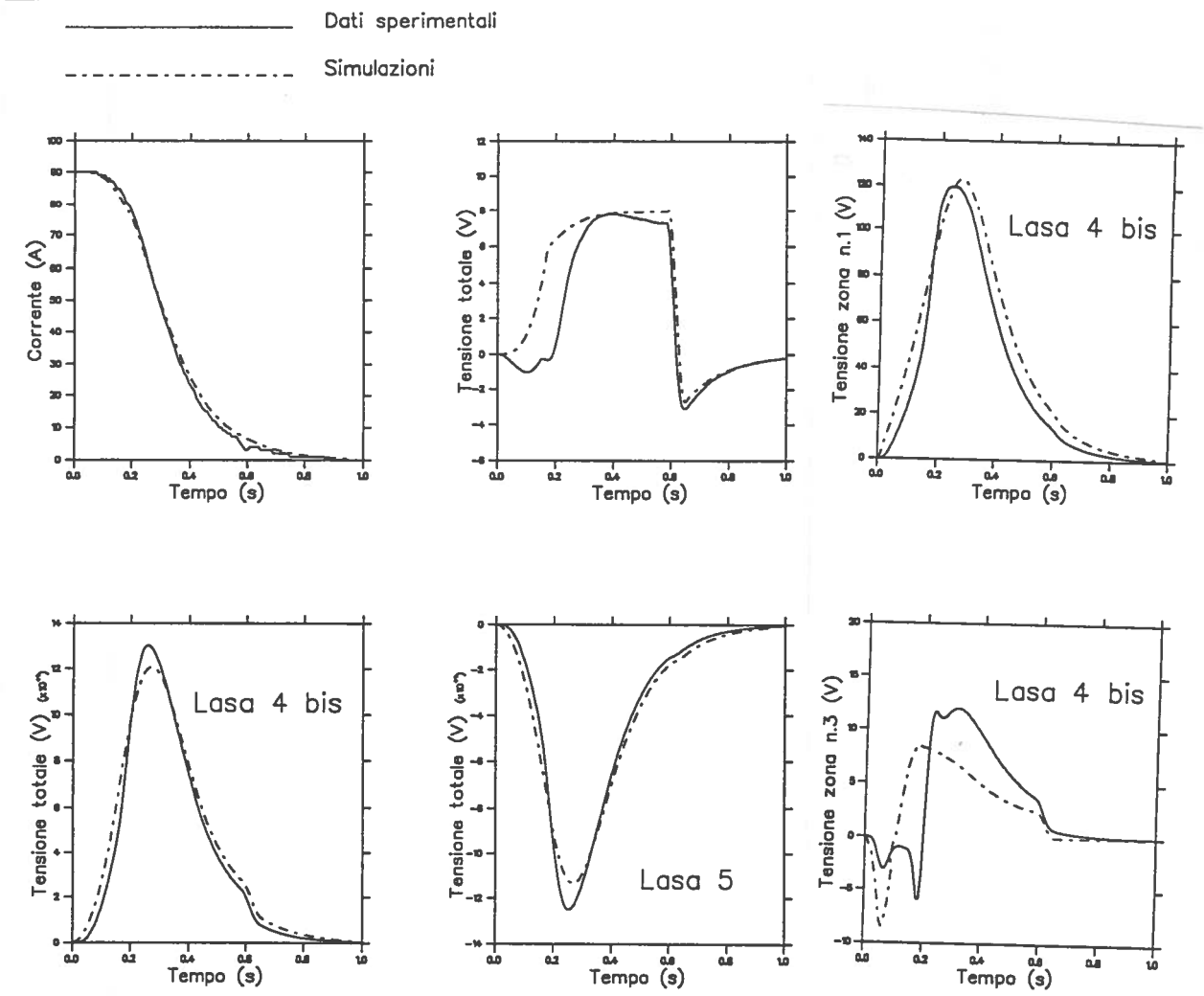

FIG. 21: Measured (solid lines) and computed (dashed) current decay and voltage during a quench of Lasa4–Lasa5 at I=90 A.

LIST OF SYMBOLS

- B Magnetic field
- C Specific heat
- Hm Coil height
- I Intensity current flowing in the coil
- I_0 Intensity current at the initial time
- I_d Intensity current flowing in the dump resistor
- J Current density
- l Cable length
- L Self inductance

M Mutual inductance

Nc Number of materials in a winding

R_{in} Coil inner radius

R_{out} Coil outer radius

R_d Dumping resistance

R_q Quenched volume resistance

S Cable cross section

V Volume or Voltage

t Time

t_0 Initial time

t_i Time at the i–th temporal step

v_l Quench propagation velocity in longitudinal direction

v_r Quench propagation velocity in radial direction

v_a Quench propagation velocity in axial direction

v_t Quench propagation velocity in a direction perpendicular to the cable

γ Mass density

λ_l Thermal conductivity in longitudinal direction

λ_r Thermal conductivity in radial direction

λ_a Thermal conductivity in axial direction

λ_t Thermal conductivity in a direction perpendicular to the cable

ρ Electrical resistivity

τ_d Delay time for dumping resistor activation

τ_{arc} Arc time of circuit breaking

τ_V Time at which the generator swing from current to voltage mode

Θ Absolute temperature

Θ_0 Bath temperature

Θ_c Critical temperature

Example of input file for *Dynque*

```
'PMG1                '                          !title
1       1                                       !ncoil necoil
0.76    1.35      6.0                           !rmin, rmax, dh (cm)
0       0.76      3.0                           !timq, Rquen, yquen (cm)
9                                               ! ndr(i)
0.76  0.8375  0.9075  0.9925  1.05  1.1225  1.19  1.2625  1.35  ! R(n,j)
1       4.25                                    !ivel, the0
18.3  22.  0.0064247                            !themax, bmax,uca
0.3254   0.3424  0.0291  0.2059    12.0         !B0, Brint, Brext, B0ax,bext
-28.40  477.40                                  !caIc(n) tnIc(n)
30    2   0.0  2   2                           !amp0e , rdump, alf, ind,ivt
4                                               !nc
'COPPER  '   0.1018   150.                      !mat, frac, rrr
'TANTALUM'   0.0360  1
'NB3SN   '   0.4612   1.
'EPOGLASS'   0.4010   1.
0.0012917                                       !ame(n,j)
0.0012917                                       !am(n,j)
0.207e-4 0.163e-4  0.159e-4  0.156e-4  0.154e-4  0.150e-4  0.153e-4  0.146e-4
0.163e-4 0.235e-4  0.197e-4  0.188e-4  0.185e-4  0.180e-4  0.183e-4  0.176e-4
0.159e-4 0.197e-4  0.275e-4  0.229e-4  0.223e-4  0.216e-4  0.219e-4  0.210e-4
0.156e-4 0.188e-4  0.229e-4  0.319e-4  0.277e-4  0.261e-4  0.263e-4  0.252e-4
0.154e-4 0.185e-4  0.223e-4  0.277e-4  0.350e-4  0.299e-4  0.297e-4  0.283e-4
0.150e-4 0.180e-4  0.216e-4  0.261e-4  0.299e-4  0.379e-4  0.344e-4  0.322e-4
0.153e-4 0.183e-4  0.219e-4  0.263e-4  0.297e-4  0.344e-4  0.443e-4  0.381e-4
0.146e-4 0.176e-4  0.210e-4  0.252e-4  0.283e-4  0.322e-4  0.381e-4  0.461e-4
0.                                              !hmuts(n,j,k)
0.
0.
0.
0.
0.
0.
0.
100     0.001   1     1                         !nts, dt , ivt, iwr
0.7375  0.8711  0.090                           !alr, aly,alins (mm)
0.0  0.0 0.0  0.0  0.0  0.0  0.0  0.0           !vqds(n,j)
0.06     1.0                                    !timarc(n), deltim(n)
1                                               !nswitch(ne)
0     0.9       0.7      0.7   1                !corvri,corvre,corvhu,corvhd,corvel
4                                               !vmax1(ne)
5                                               !vmax2(ne)
3                                               !tau(ne)
1                                               !nacc(ne)
```

```
'Lasa3 / Lasa2                '                !title
2       1                                      !ncoil necoil
0.775   1.975   5.95                           !rmin, rmax, dh (cm)
2.25    3.70    10.
10      0.775      2.975                       !timq, Rquen, yquen (cm)
0.      2.25    5.
3       5                                      ! ndr(i)
0.775   1.375     1.975                        ! R(n,j)
2.25    2.696   3.031   3.365   3.70
1       4.2                                    !ivel, the0
18.3  22.  0.006761                            !themax, bmax,uca
9.2   14.5  0.003132
1.8197    1.8207   0.0674    1.1396  0        !B0, Brint, Brext, B0ax,Bext
4.5049    4.5435   0.4041    2.7828
-28.40    477.40                               ! caIc(n) tnIc(n)
-39.257   408.25
90    0.2    0.5   2   1                      !amp0e , rdump,alf,ind,ivt
4       3                                      !nc
'COPPER  '    0.0967   150.                    !mat, frac, rrr
'TANTALUM'    0.0342   1
'NB3SN   '    0.4382   1.
'EPOGLASS'    0.4309   1.
'COPPER  '    0.3600    150.
'NBTI    '    0.2665    1.
'EPOGLASS'    0.3735    1.
0.56187                                        !ame(n,j)
0.00857         0.0318                         !am(n,j)
0.0318         0.4897
0.00160         0.00167                        !hmut(n,i,j)
0.00167          0.00356
0.0383  0.0288  0.0277  0.0269
0.0288  0.0286  0.0283  0.0274
0.0277  0.0283  0.0349  0.0346
0.0269  0.0274  0.0346  0.0405
0.  0.0095                                     !hmuts(n,j,k)
0.  0.0223
0.0103  0.
0.00739  0.
0.00715  0.
0.00696  0.
100     0.01    1    1                        !nts, dt (inserire)
0.75   0.9015   0.1                            !alr, aly,alins (mm)
0.5577  0.5618  0.058
0.0  0.0
0.0  0.0   0.0   0.0                          !vqds(n,j)
0.06     0.49                                  !timarc(n), deltim(n)
1                                              !nswi(ne)
1       1       1       1       1              !corvri,corvre,corvhu,corvhd,corvel
0       0.27    0.39    0.39    1
3.7                                            !vmax1(ne)
5.7                                            !vmax2(ne)
0.49                                           !tau(ne)
2                                              !nacc(ne)
```